Front. Earth Sci. 2021, 15(2): 202–223
https://doi.org/10.1007/s11707-020-0833-1

REVIEW ARTICLE

Petrophysics characteristics of coalbed methane reservoir: a comprehensive review

Qifeng JIA[1,2], Dameng LIU (✉)[1,2], Yidong CAI[1,2], Xianglong FANG[1,2], Lijing LI[1,2]

1 School of Energy Resources, China University of Geosciences, Beijing 100083, China
2 Coal Reservoir Laboratory of National Engineering Research Center of CBM Development & Utilization, China University of Geosciences, Beijing 100083, China

Abstract Petrophysics of coals directly affects the development of coalbed methane (CBM). Based on the analysis of the representative academic works at home and abroad, the recent progress on petrophysics characteristics was reviewed from the aspects of the scale-span pore-fracture structure, permeability, reservoir heterogeneity, and its controlling factors. The results showed that the characterization of pore-fracture has gone through three stages: qualitative and semiquantitative evaluation of pore-fracture by various techniques, quantitatively refined characterization of pore-fracture by integrating multiple methods including nuclear magnetic resonance analysis, liquid nitrogen, and mercury intrusion, and advanced quantitative characterization methods of pore-fracture by high-precision experimental instruments (focused-ion beam-scanning electron microscopy, small-angle neutron scattering and computed tomography scanner) and testing methods (μ-CT scanning and X-ray diffraction). The effects of acoustic field can promote the diffusion of CBM and generally increase the permeability of coal reservoirs by more than 10%. For the controlling factors of reservoir petrophysics, tectonic stress is the most crucial factor in determining permeability, while the heterogeneity of CBM reservoirs increases with the enhancement of the tectonic deformation and stress field. The study on lithology heterogeneity of deep and high-dip coal measures, the spatial storage-seepage characteristics with deep CBM reservoirs, and the optimizing production between coal measures should be the leading research directions.

Keywords petrophysics, pore-fracture, permeability, heterogeneity, controlling factors

Received June 30, 2020; accepted August 31, 2020

E-mail: dmliu@cugb.edu.cn

1 Introduction

Coal petrology is the theoretical basis of coalbed methane (CBM) exploration and development, transformation and stimulation, and sustainable development of the industry (Jiang et al., 2016). As the source rock and storage carrier of hydrocarbon gas, the coal reservoir contains special properties such as multiscale pores and fractures, large specific surface area, and conductive medium capacity, which enable CBM to be produced effectively (Fan et al., 2010; Akhondzadeh et al., 2020). The petrological characteristics of CBM reservoirs are mainly reflected in the aspects of pore-fracture, permeability, reservoir heterogeneity, genesis mechanism, and mechanical properties (Ahmad et al., 2019; Cai et al., 2019). Many international scholars have studied the petrophysics characteristics of CBM reservoirs, mainly in the aspects of pore-fracture, permeability, and heterogeneity. Pores and fractures are crucial spaces for CBM adsorption, migration, and occurrence, in which matrix pore is the CBM occurrence space, macro-fracture is the migration channel, and micro-fracture is the bridge between pore and macro-fracture (Liu et al., 2018a; Wang et al., 2019). The geological conditions of coal reservoirs in China are more complicated than those in the United States, Australia, and Canada (Yang et al., 2019c; Lupton et al., 2020). The sedimentary environment controls the porosity and pore configuration of high-rank coal reservoirs in the Qinshui Basin. Due to the intense and frequent evolutions of coal facies, the difference in the development of pore systems between the northern and southern coal reservoirs is vast. The porosity of the southern coal reservoirs is generally about 0.5% larger than that of the northern coal reservoirs (Yao et al., 2010a). The difference in the transverse and vertical macerals in the north-west and north China leads to the strong anisotropy in the development of coal seam micro-fractures, and the high porosity of coal with low

metamorphism and intense deformation (Liu et al., 2018a; Yang et al., 2018; Wang et al., 2019). Reservoir permeability is one of the hot topics in the study of petrophysics characteristics. The change of permeability is controlled by many factors, among which the effective stress and matrix shrinkage-swelling are the two main factors (Jiang et al., 2010; Zhao et al., 2018). Generally, the permeability of coal reservoir is high in the region with small stress difference and decreases sharply with the increase of depth. Matrix shrinkage-swelling and the change of effective stress lead to the elastic self-regulation effect of coal reservoir, which makes the permeability first increase and then decrease with the increase of coal rank in the process of drainage (Cai et al., 2014; Fang et al., 2018). The effects of fracturing, nitrogen injection and acoustic field are often used to improve the permeability in the field construction process. The CBM reservoirs show substantial heterogeneity in micro, plane, in-layer, and inter-layer (Zhang et al., 2018). The degree of heterogeneity in the coal reservoir parameters ranges from strong to weak in the order of adsorption time, mineral content, the total density of micro-fracture, total density of macro-fracture, inertinite content, vitrinite content, gas content, and maximum vitrinite reflectance (Li et al., 2016b). Using scanning electron microscopy (SEM), small-angle X-ray scattering (SAXS), computed tomography (CT), and combining theory with practice, some scholars have researched the field of petrophysics characteristics (Hoffman and Caers, 2005; Ju et al., 2005; Cai et al., 2013; Yang et al., 2015; Clarkson and Qanbari, 2016). There are many factors affecting reservoir geology, and the control mechanism is complicated, especially the production layer combination for CBM development under the condition of joint coal seams (Yang et al., 2019a). Moreover, the main control factors, accumulation mechanisms, physical characteristics, and production mechanisms of each coal block are different (Scott, 2002; Majdi et al., 2012; Mazumder et al., 2012). The coal reservoirs in China were characterized by low porosity, low permeability, and high heterogeneity. The exploitability and development technology of CBM reservoirs are closely related to the study of petrophysics characteristics (Prinz et al., 2004; Yao and Liu, 2012; Ibrahim and Nasr-El-Din, 2015). Previous studies on the petrophysics characteristics of CBM reservoirs have achieved fruitful results (Hodot, 1966; Prinz et al., 2004; Yao and Liu, 2012), but there is a lack of systematic summary after the mature technology of exploration and development.

Based on the analysis of many works of literature and the combination of theory and practice, the author summarizes the research of petrophysics characteristics in the field of CBM in recent years. The reservoir heterogeneity and the coal petrographic front direction are explored to provide guidance for abundant reservoir geology theory and breakthrough in exploration technology.

2 Pores and fractures in CBM reservoir

2.1 Classification and characterization methodology

2.1.1 Pores and fractures classification

The pores and fractures in coal reservoirs are the crucial places for CBM production, enrichment, seepage, and diffusion. Refining the classification of pores and fractures is essential for the subtle characterization of reservoir. Based on the mercury injection experiment and fractal calculation, and combining with the characteristics of methane diffusion and seepage, Fu et al. (2005) divided the coal pores into diffusion (<65 nm) and seepage pores (>65 nm), further dividing the diffusion pores into micro (<8 nm), transitional (8–20 nm) and small pores (20–65 nm), and the seepage pores into medium (65–325 nm), transitional (325–1000 nm) and large pores (>1000 nm). Su et al. (2002) conducted SEM tests on coal samples from Jincheng, Pingdingshan, and Yima divided the fractures into meshy, solitary and superimposed internal fractures, and exogenous fractures such as tensile, shear, tension-shear, and cleavage according to their genesis and morphology. Based on nuclear magnetic resonance analysis, Yao et al. (2010b) believed that microfractures were those with a diameter greater than 1000 nm, and divided them into four types: A, B, C, and D. Among them, type A had strong ductility and excellent continuity, type B was similar to the dendritic trunk, type C had strong ductility and general continuity, and type D had poor connectivity and limited direction. The mercury intrusion method was utilized by Zhang et al. (2009) to evaluate the pore size characteristics of coals in the Qinshui Basin. The result indicated that the pore system was composed of seepage and condensation-adsorption pores. The former was mainly primary and metamorphic pores, and the latter was mainly some metamorphic pores undergoing deformation and transformation. To better study the influence of gas adsorption and flow capacity on pore-fracture, Cai et al. (2013) adopted a joint classification method to classify pores and fractures into super-micropores (<2 nm), micropores (2–10 nm), mesopores (10–10^2 nm), macropores (10^2–10^3 nm), super-pores (10^3–10^4 nm) and microfractures ($>10^4$ nm). Micropores and mesopores, as part of the coal matrix, provide a vast internal surface area, and have a strong affinity for CH_4 and CO_2. Ju et al. (2005) used X-ray diffraction and high-resolution transmission electron microscopy to analyze coal pores and macromolecular structures. The pore structure in the tectonic coal was divided into extreme micropores (<2.5 nm), submicron pores (2.5–5 nm), micropores (5–15 nm), and transition pores (15–100 nm). The volume of extremely micropores, submicron pores, and micropores increases obviously with the enhancement of structural deformation, while the volume of transition pores decrease. Based on the measured pore data of 50 samples in typical 16 mining

areas, Qin et al. (1995) proposed a natural classification scheme for high-rank coal pores, which was divided into micropores, transition pores, mesopores, and macropores with the boundaries of 15, 50 and 400 nm respectively. There is no universal classification scheme for coal pores and fractures. Due to the multi-phase, diversity, and variability of the coal forming environment in China, the pores and fractures of coal reservoir have substantial heterogeneity, so it is necessary to adopt specific classification schemes according to the coal quality characteristics in different regions. At present, the classification scheme of IUPAC is widely used in the world. The pores of coal can be divided into micropore ($D < 2$ nm), mesopore (2–50 nm), and macropore ($D > 50$ nm) (IUPAC, 1972).

2.1.2 Characterization methodology

The characterization of pore-fracture in coal reservoir has gone through three stages: qualitative and semiquantitative evaluation of pore-fracture by various techniques, quantitatively refined characterization of pore-fracture by integrating multiple methods including nuclear magnetic resonance analysis, liquid nitrogen, and mercury intrusion, and advanced quantitative characterization methods of pore-fracture by high-precision experimental instruments (focused-ion beam-scanning electron microscopy, small-angle neutron scattering and computed tomography scanner) and testing methods (μ-CT scanning and X-ray diffraction). These three stages are crucial to reveal the mechanism of CBM occurrence and migration. Image analysis, fluid injection, and non-fluid injection were used to characterize the coal pores and fractures. The non-fluid injection method has a broad application prospect for the study of pore-fracture evolution.

The image analysis method is mainly to observe the pores and fractures through the scanning electron microscope, transmission electron microscope, atomic force microscope, and other instruments, and to characterize the morphology, size, connectivity, arrangement, and combination of pore-fracture utilizing a large number of SEM images of coal reservoirs (Zhao et al., 2019). Figures 1 and 2 show a series of consecutive SEM images of the bituminous (BC) and anthracite (AC) coal samples during the focused-ion beam (FIB) section progress, respectively. For the BC sample, a few isolated pores were developed in the coal matrix, and many of them were organic-matter (OM) pores. OM pores are elliptical and slit-shaped with pore sizes ranging from ~25 nm to 600 nm, and are mainly distributed independently within OM and partial pores filled with minerals (Figs. 1(a) and 2(b)). Compared to the BC sample, a large number of gas pores were widely developed in the AC sample, which is generally circular or elliptical with smooth edges and originated from gas generation during coalification (Figs. 2(a)–2(d)). It can be seen that the gas pores merge to form large clusters with pore sizes generally varying from several to more than 100 nm and are interconnected with each other, which is conducive to gas storage and diffusion capacity in coals (Li et al., 2017c). According to Harpalani and Zhao's analysis, the coal pores are granular, fibrous, spongy, and irregular (Harpalani and Chen, 1995; Zhao et al., 2014). The inertinite mainly developed mesopores, while the vitrinite mainly developed small pores and micropores, and most of the micropores were not connected. The microfractures are perpendicular to the layer under the SEM, which are mainly produced in the microstrip composed of homogeneous and structural vitrinite. The microfractures connecting some residual pores connect many independently developed micropores to form the pore-fracture system of coal reservoir and become the main channel of diffusion-seepage (Pillalamarry et al., 2011; Cai et al., 2018; Li et al., 2020c). The difference in microfractures density and development morphology leads to a significant difference between endogenous and exogenous fractures. Generally, the density of exogenous fractures is vast than that of endogenous fractures, which can be used to judge the existence of tectonic coal and the degree of tectonic development (Li et al., 2017c; Li et al., 2019a; Li et al., 2019b).

The fluid injection method mainly injects N_2/CO_2 or liquid into the coal sample under different pressure conditions. Based on different mathematical models, the specific surface area, pore-volume, and size distribution of the experimental sample are obtained according to the injection-adsorption amount. Jiang et al. (2011) analyzed the results of the low-temperature liquid nitrogen test and believed that the specific surface area, pore-volume, total pore specific surface area, and total pore volume of micropores all showed an increasing trend with the increase in the degree of coal destruction. Moreover, the adsorption-desorption curve of primary structural coal is roughly parallel. When the relative pressure is 0.5, a slight inflection point appears in the desorption curve of fragmented coal. Mylonitic coal increases with the increase of pressure, and the adsorption-desorption curve rises slowly. Yao et al. (2010b) conducted saturation and centrifugal spectrum tests on different coal ranks and found that the NMR relaxation time of 0.5–2.5 ms, 20–50 ms, and greater than 100 ms correspond to the distribution characteristics of micropores, large pores, and fractures, respectively. The porosity and pore size distribution of coal samples can be obtained according to the correlation between the cutoff value T_2 and the centrifugal radius (Yang et al., 2019b). The method of nuclear magnetic freezing-thawing pore measurement can more accurately characterize the pore structure of porous materials, which has distinct advantages in the quantitative identification of total pores. The pore size measurement range is from 2 nm to 1000 nm, which has a considerable perspective in the pore size distribution, pore morphology characteristics, and liquid-matrix surface interaction (Guo et al., 2016).

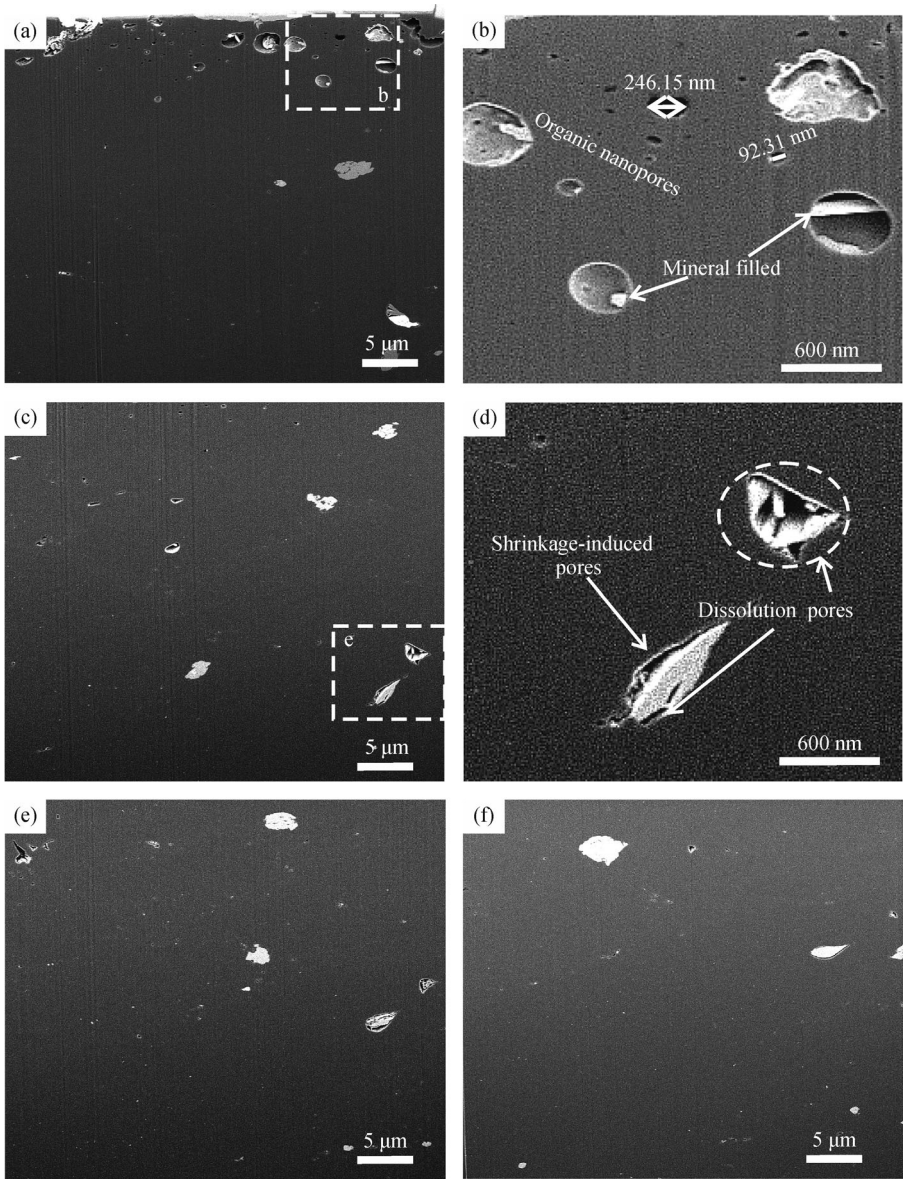

Fig. 1 SEM images by sequential FIB showing the 2-D pore-fracture structure of BC sample. (a) image of 1st FIB slice; (b) the partial enlarged image of (a); (c) image of 201st FIB slice; (d) the partial enlarged image of (c); (e) image of 401st FIB slice; (f) image of 599th FIB slice (Li et al., 2017c).

The non-fluid injection method is an efficient non-destructive scanning technique (such as small-angle X-ray scattering, focused-ion beam-scanning electron microscopy, computed tomography) to reveal and characterize the pore information. CT and SEM have a very high degree of coincidence in the identification of the same fracture morphology and development scale in coal (Fig. 3), which can show the three-dimensional spatial distribution of pores and fractures, and characterize the pore-fracture with the pore diameter greater than 12.40 μm in the coal sample (d = 19.20 mm, h = 10.59 mm) (Song et al., 2018). Compared with the fluid injection method, SAXS can obtain the information of closed pores, pore size distribution, and coordination number, and the characterization of coal pore-fracture is not affected by pore connectivity, shielding effect, and surface tension. Focused-ion beam-scanning electron microscopy (FIB-SEM) can avoid new pores during sample preparation and truly restore the spatial configuration of nanometer pores. Besides, μ-CT scanning combined with X-ray diffraction cannot only conduct 3D visual and quantitative characterization of pore-fracture size, morphology, and spatial distribution but also accurately display mineral development characteristics, filling conditions and spatial distribution rules

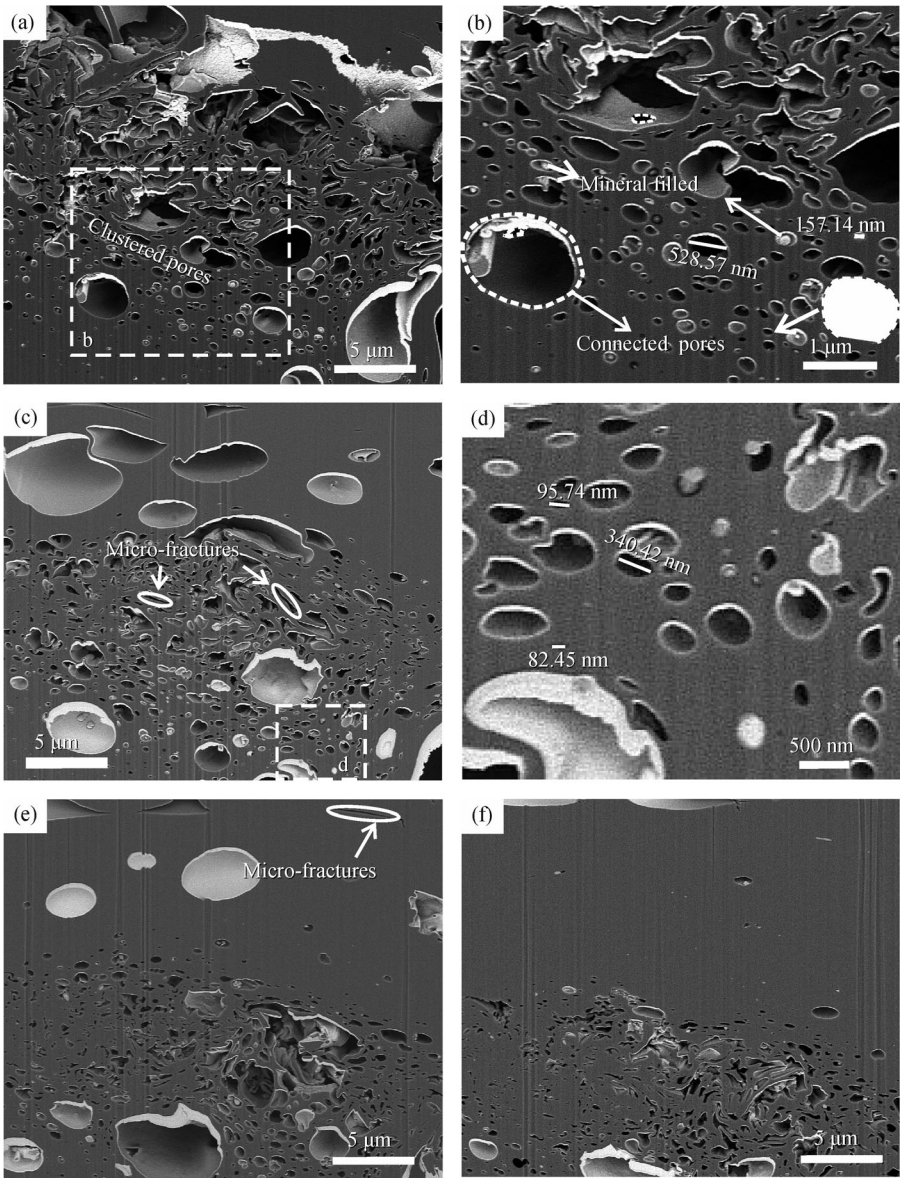

Fig. 2 SEM images by sequential FIB showing the 2-D pore-fracture structure of AC sample. (a) image of 101st FIB slice; (b) the partial enlarged image of (a); (c) image of 301st FIB slice; (d) the partial enlarged image of (c); (e) image of 501st FIB slice; (f) image of 701st FIB slice (Li et al., 2017c).

(Salmachi and Karacan, 2017). The characterization methods of pores and fractures in different scales show in Fig. 4. Based on the detailed description of pore-fracture by various methods, a set of theories of 3D reconstruction characterization for coal reservoir is developed.

2.2 Multiscale structure of pores and fractures

During coal formation, the development of matrix pores with large specific surface area provides the storage space for CBM. Endogenous and exogenous fractures serve as the main channel for CBM migration. The individual differences of plant remains and multi-phase structure movement have resulted in differences in pore size, structure, and spatial distribution. Studying the development and evolution characteristics of pore-fracture is of great significance for clarifying the diffusion-seepage mechanism and reservoir corporality character.

The microfractures have various shapes, such as reticulate, dendritic, oblique, and solitary. The reticulate and dendritic microfractures increase with the development density (Li et al., 2017c). Endogenetic fracture mineral filling is relatively few, mostly perpendicular to bedding, with excellent directivity, and widely developed in homogeneous vitrinite. Part of it penetrates fusinite and sporophyte, which can distinguish X intersecting or orthogonal primary/secondary fracture (Karacan, 2013). Yao and Liu believed that the development of endogenous

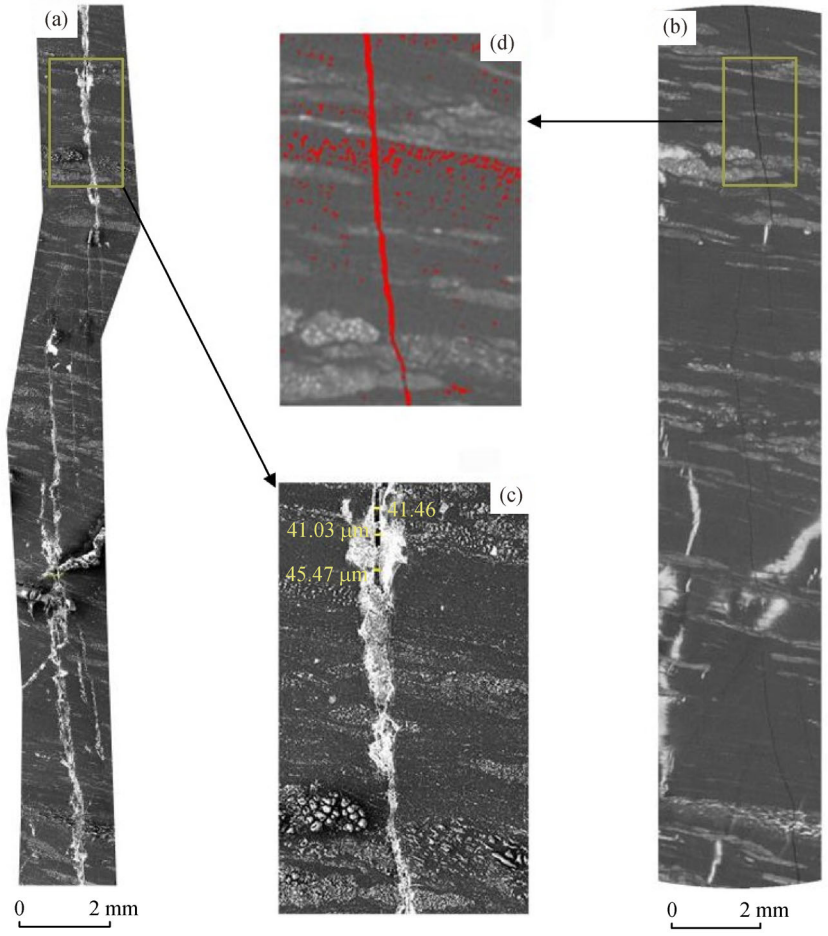

Fig. 3 Comparison of fracture recognition between SEM and CT slice images. (a) Fractures in SEM images; (b) fractures in the CT section; (c) an enlarged view of local fractures in SEM; (d) an enlarged local view of a CT section (Song et al., 2018).

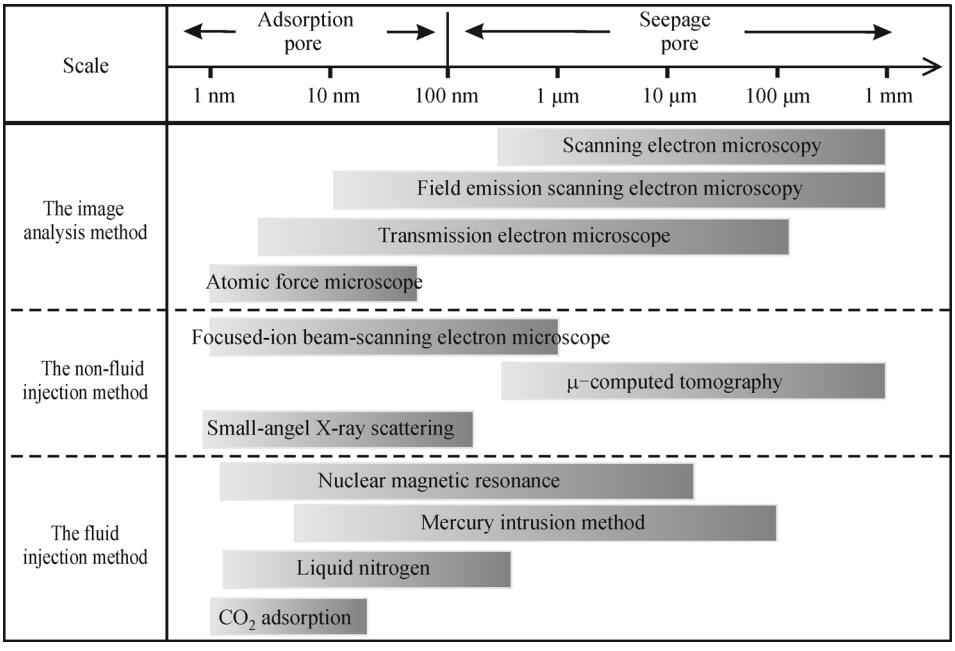

Fig. 4 A schematic diagram of the characterization methods of pores and fractures in different scales (Yu et al., 2020).

microfractures was constitutionally selective, and put forward the hypothesis of "gas accumulation-volume expansion-fracture," holding that the composition selection was caused by the generation, accumulation, and drainage of hydrocarbon gases (Yao and Liu, 2012). The development of exogenous fractures is mainly controlled by tectonic stress and has strong heterogeneity. Generally, the macerals of coal are damaged or run through, to enhance the connectivity of micro-fractures and improve the permeability of reservoirs. The exophytic fracture has poor directivity and is inclined to cross with coal layers at various angles, and sometimes overlaps with the endogenous fractures (Jiang et al., 2010). In general, there are many extraneous tensile fractures in the vicinity of normal faults, with broad and straight openings, and sometimes they run through each other to form irregular reticular fracture networks. Closed compression fractures are often developed with a small width and a relatively consistent extension direction in the vicinity of thrust faults. Due to the action of the multi-stage tectonic movement, the compression fracture will also break and extend along with multiple directions (Harpalani and Chen, 1995; Hou et al., 2017).

The thermal effect is an essential factor that affects the molecular and pore structure characteristics of coal and causes the coal reservoir pore-fracture space configuration to change accordingly, which significantly affects on coal pore and morphology changes (Cai et al., 2014). The weight loss of coal is related to organic decomposition and gas production during pyrolysis. Major gases generated during coal pyrolysis show in Fig. 5 (Li et al., 2015), including H_2O, H_2, CH_4, CO, CO_2. The extensive evolution of gases happens in the temperature range of 300°C to 800°C. The characteristics of pore evolution under thermodynamic action are analyzed, and the morphology characteristics of pores at different temperatures are characterized by SEM. The results show that the pore morphology changes little with the increase of temperature, and the pore diameter increase with the

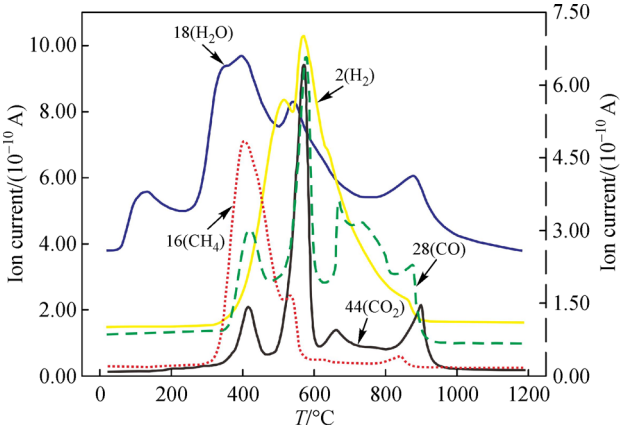

Fig. 5 Evolution curves of gaseous products of the coal sample with elevated temperatures by mass spectrometry (Li et al., 2015).

evaporation when the temperature is lower than 200°C (Figs. 6(a)–6(d)). The scale structure appears at the interface, and the pore diameter and volume increase significantly after reaching 400°C (Figs. 6(e) and 6(f)). The pore volume increases significantly with the production of a large number of gas pores, and the surface of the coal matrix is spongy, accompanied by coking after reaching 600°C (Figs. 6(g) and 6(h)). Improving pore morphology and structure through heating up can be considered to promote CBM production.

3 Permeability quantification of CBM reservoir

3.1 Quantification methodology

The traditional means obtaining permeability include 3D seismic data, core analysis, well test. The principle of determining permeability based on 3D seismic data is the correlation between permeability and porosity, and the permeability often increases with the increase of porosity (Yao et al., 2009). The reservoir can be regarded as a two-phase medium filled with fluid. The instantaneous force generated by the earthquake source excitation will produce a pressure gradient field, which will cause the change of reservoir volume and promote the relative movement of pore fluid (Li et al., 2015). The seismic record is a general reflection of the medium's microscopic fluctuations on the surface, reflecting the changing rule of the reservoir's physical property space. However, the test accuracy of deep coal seam is low due to the sophisticated seismic attributes and the interferences of multiple factors. Core analysis is to measure the absolute permeability by coring the target layer and cleaning the core. Usually, the coring is carried out along the vertical direction of the wellbore, and the actual measurement is often used to acquire the permeability of the core along the vertical direction of the reservoir. However, core analysis can no longer represent the seepage capacity of the whole coal reservoirs for coal reservoirs with substantial heterogeneity, so it must be combined with other dynamic data for comprehensive analysis (Li et al., 2020a). The well test technology is an essential method to understand CBM reservoirs, monitor production performance, and evaluate completion efficiency, which is divided into stable and unstable well testing. The stable well test establishes the well's productivity equation, while the unstable well test is to determine the permeability and other physical characteristic parameters of the coal reservoir (Ni et al., 2019). Although the well test is highly accurate, it is expensive to test the permeability of each well in the same block, which is very limited for highly heterogeneous reservoirs.

The geological strength index (GSI) is introduced to obtain the permeability of coal reservoir to avoid the disadvantages of the above test methods. Since coal is a

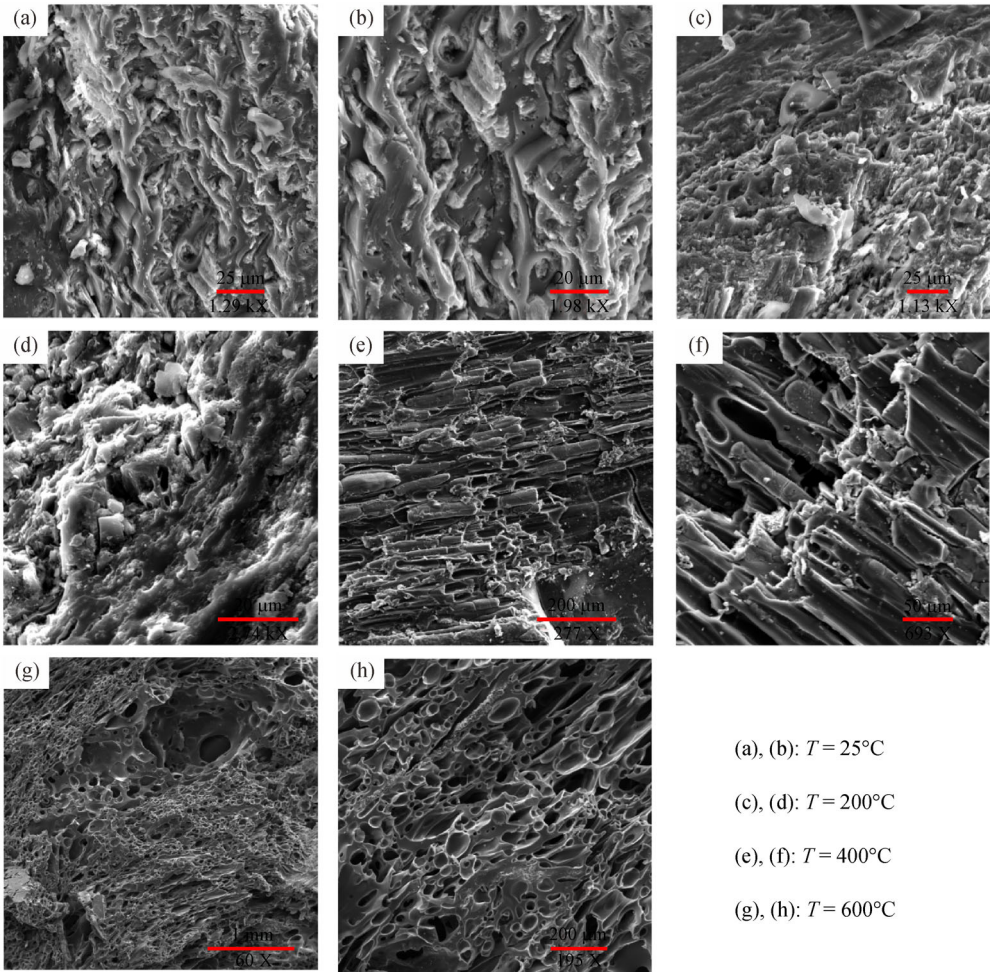

Fig. 6 Evolution characteristics of pore structure at different temperatures (Li et al., 2017c).

particular rock, the matrix block corresponds to the lumpiness in the classification of the rock mass, and the fracture width and filling condition replace the weathering condition of discontinuous surfaces. Therefore, it is theoretically possible to obtain permeability with GSI (Guo et al., 2010; Jia et al., 2019). By observing the coal structure of 20 CBM parameter wells and calibrating the sampled coal cores, the relationship model between logging parameters and GSI was established (Eq. 1).

$$\mathrm{GSI} = 72.9\mathrm{DEN} + 1.2\mathrm{GR} - 6.9\mathrm{CAL}X + 6.5\mathrm{CAL}Y - 77.6, \quad (1)$$

where DEN is the compensated density, g/cm^3; GR is natural gamma, API; CALX and CALY are well diameter X and Y, cm, respectively.

GSI calibration was carried out on the coal core of the drilling sample in Shizhuang block of Qinshui Basin by using typical logging parameters such as compensated density, natural gamma, well diameter, structural surface characteristics (Fig. 7). The relationship model between GSI and permeability was established based on the existing well test data (Eq. 2).

$$k = 0.0078 + 1.0027\mathrm{e}^{(-0.0106(\mathrm{GSI}-55.0272)^2)}, \quad (2)$$

where k is permeability, mD; e is a constant, which is approximately 2.72.

GSI and permeability were normally distributed. When the GSI value is 55.03, the permeability is the maximum. If the coal seam is too complete or broken, the permeability decreases instead (Fig. 8). The different rank coals have diverse permeability variation with the increase of flow velocity, but the overall trend of permeability reduction with the increase of flow velocity for all samples is consistent except sample A damaged at 1.5 mL/min (Fig. 9). Also, the permeability damage rate at different flow velocities was depicted in Fig. 10. The results show that most samples' permeability was damaged at the high flow velocity, while samples A and E were not damaged due to the limited flow velocity (Liu et al., 2018b). Figure 11 shows that the $R_{o,m}$ exhibits no significant relationship with effective diffusion coefficient and permeability.

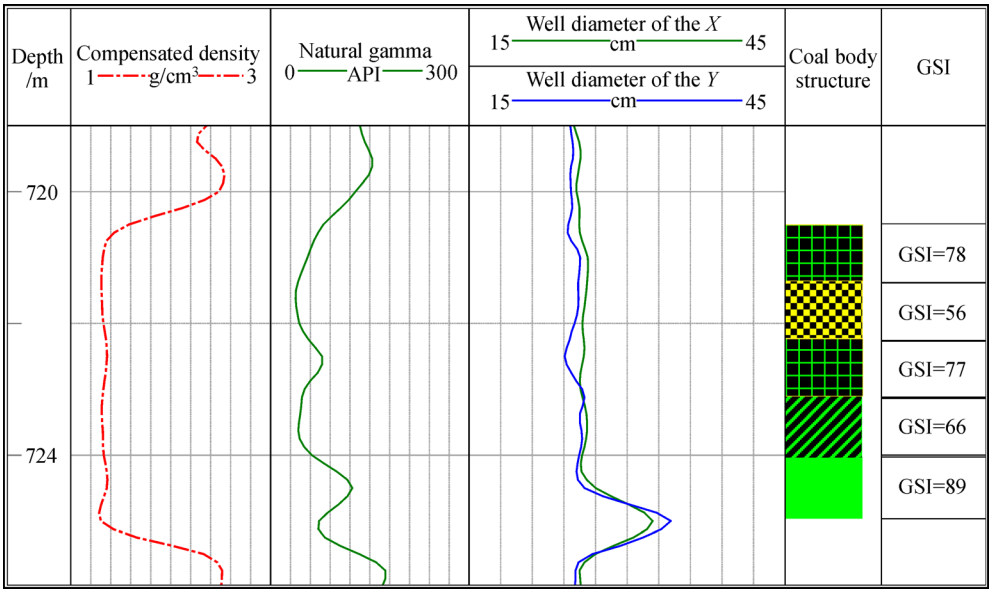

Fig. 7 The corresponding value of logging curve and GSI (Ni et al., 2019).

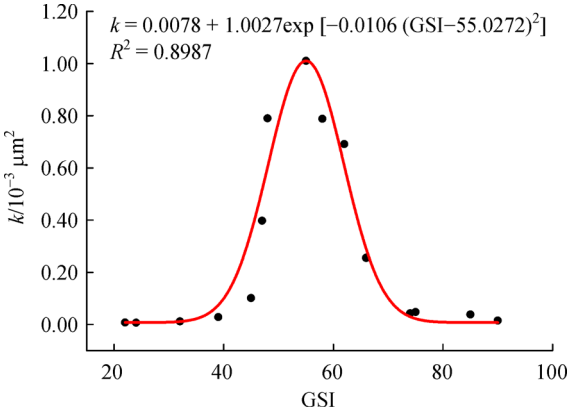

Fig. 8 Curve of fitting relationship between GSI and permeability (Ni et al., 2019).

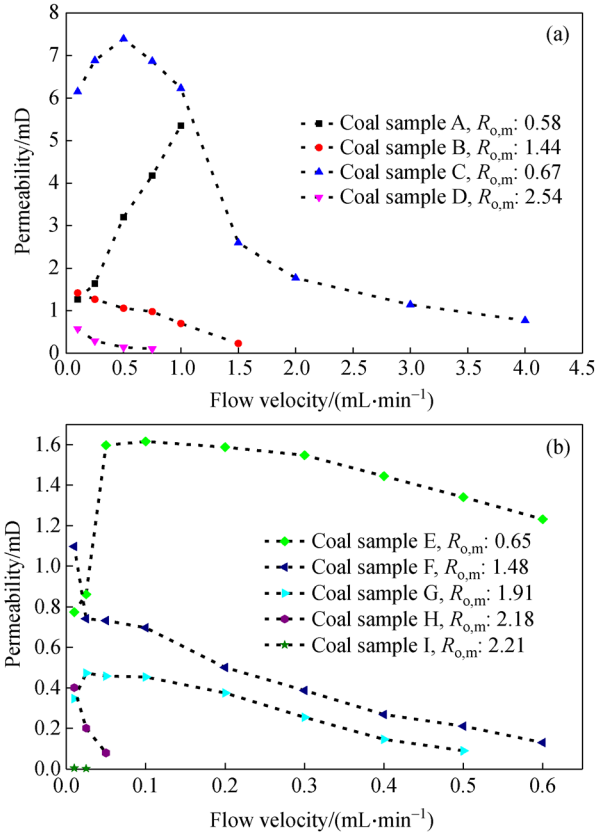

Fig. 9 Relationship between flow velocity and core permeability (a high velocity sequence; b low velocity sequence) (Liu et al., 2018b).

However, there is a subtle exponential relationship with the coefficient of determination (R^2) of 0.41 between permeability and diffusivity as shown in Fig. 12. Moreover, the unipore model correlates well with the experimental curve for CH_4 adsorption (Fang et al., 2018), and the pressure decreases rapidly within the initial 1000s, and then the diffusion process approaches the equilibrium state gradually (Fig. 13).

3.2 Permeability of CBM reservoir and its controlling factors

Reservoir permeability is the ability of pore-fracture to conduct medium, which reflects the property of coal seam to allow fluid to connect with pores (Li et al., 2014; Zhao et al., 2018). As a critical parameter of CBM development, its advantages and shortcomings reflect the development, openness, and connectivity of pore-fracture in the reservoir. Permeability is closely related to gas production (Yao et al., 2009). The coal reservoirs with high

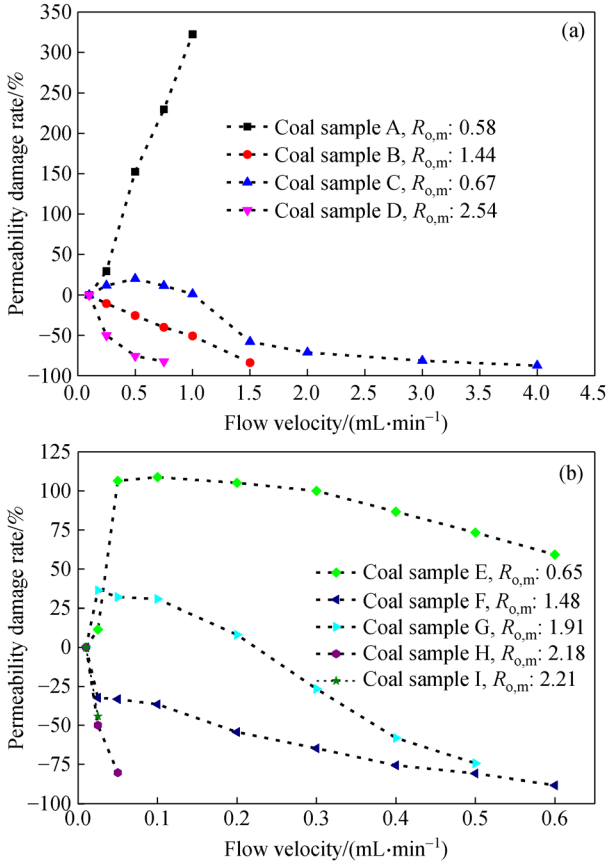

Fig. 10 Change of permeability damage rate at different flow velocities (a high velocity sequence; b low velocity sequence) (Liu et al., 2018b).

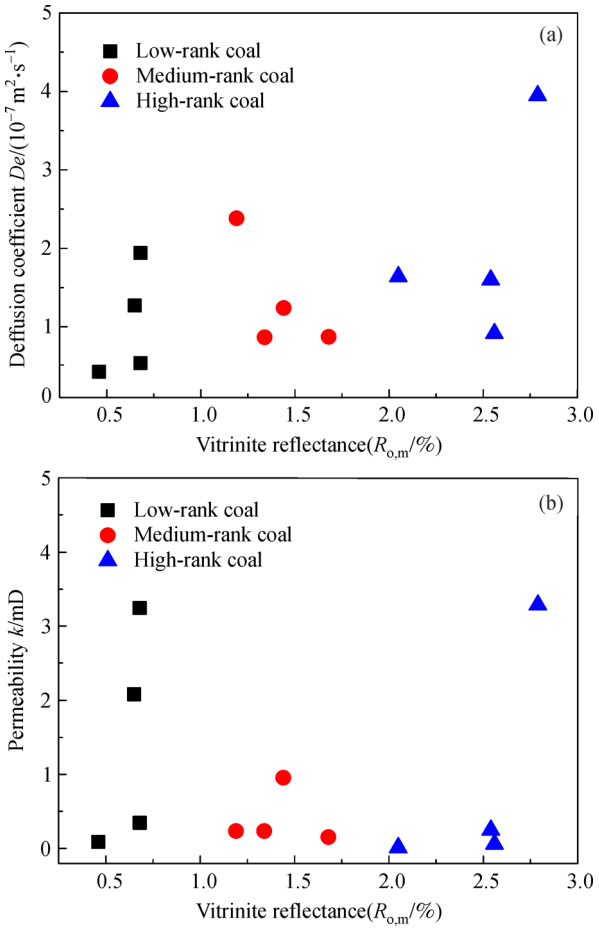

Fig. 11 Diffusion coefficient and permeability for the low, medium, and high rank coals. (a) Diffusion coefficient for the low, medium, and high rank coals; (b) Permeability for the low, medium, and high rank coals (Fang et al., 2018).

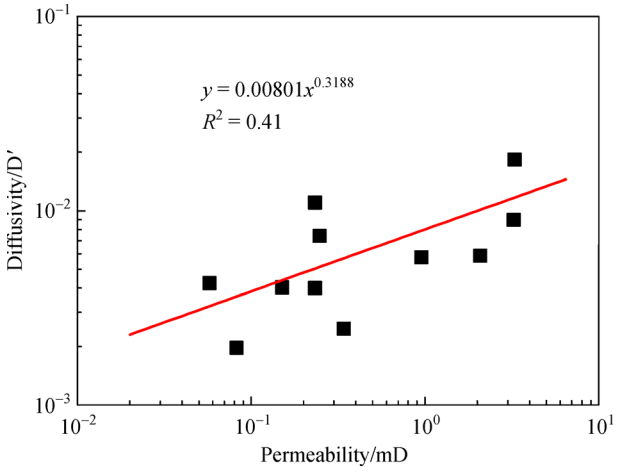

Fig. 12 Diffusivity vs. permeability for the different rank coals (Fang et al., 2018).

permeability have higher gas production. The reservoir permeability and average gas production per well in China's CBM blocks show in Table 1. When reservoir permeability is less than 0.01 mD, the average gas output per well is difficult to reach 1000 m^3/d. More horizontal wells are distributed than vertical wells in blocks with permeability exceeding 2 mD.

Permeability is controlled by a variety of geological factors (such as throat shape and size, coal quality, formation pressure, tectonic stress, coal facies), in which tectonic stress and coal facies jointly determine the distribution characteristics of tectonic coal both horizontally and vertically (Hoffman and Caers, 2005). Jiang et al. (2016) obtained the geological stress data based on the logging information and the Anderson model and found that the vertical stress was conducive to the fracture opening and connection. Yang et al. (2015) thought that the principal horizontal stress increased linearly with the increase of depth, and the current geological stress and permeability followed a negative exponential function, and the matrix stress could be used to explain the permeability change caused by adsorption and desorption of CBM. Ni et al. (2019) believed that the interaction between the paleotectonic and the present tectonic stress led to the complex change of the relationship between geological stress and permeability. The relationship between the stress difference and permeability was not apparent when the

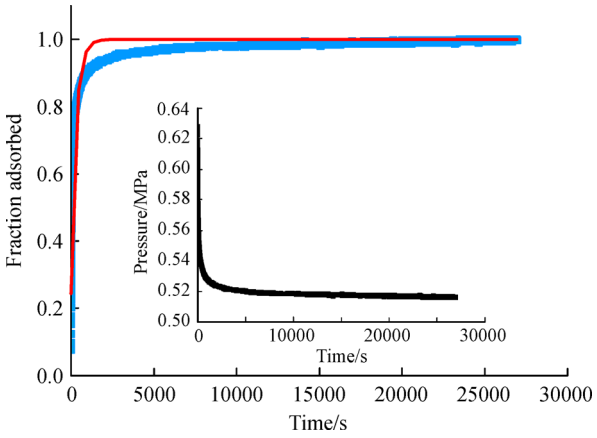

Fig. 13 Experimental and unipore model fitting curves of adsorption kinetics of CH_4 adsorption on various coals (Fang et al., 2018).

tectonic superposition zone was not divided. The permeability increased exponentially with the increase of the stress difference after the tectonic superposition zone was divided. However, the growth trend of different superposition zones was different. For the deep coal reservoir, the influence of tectonic stress will be more complicated. When the stress enters the elastic-plastic stage, new microfractures may occur in the reservoir. The closer to the stress peak, the more microfractures are generated, resulting in a sharp increase in permeability, which increases to the maximum in the plastic flow stage and then decreases (Li et al., 2016b).

3.3 Methodologies for improving CBM reservoir permeability

The common minerals in coal seam include clay, quartz, carbonate, pyrite. These minerals can be widely distributed on the surface of coal seam pores and fractures, resulting in low permeability of coal reservoir. Besides, during the well drilling and completion process, drilling fluid and cement slurry can enter the natural fracture and harm the coal seam, thereby reducing the permeability of the coal seam near the wellbore. The permeability of coal reservoirs in China is generally low, and reservoir reformation must be carried out to increase the permeability (Jiang et al., 2010).

The traditional hydraulic fracturing method cannot meet the increasing industrial demand, so other effective methods must be adopted to improve the reservoir

Table 1 The reservoir permeability and average gas production per well in China's CBM blocks

Blocks	Working seam	The era of coal seam	R_o–R_{max} /%	Burial depth /m	Permeability /mD	Average gas production per well /($m^3 \cdot d^{-1}$)	Remarks
Jincheng	No. 3 and 15	C—P (Shanxi Formation, Taiyuan Formation)	2.5–3.5	400–1200	0.01–2	1420 (Well ZY-285); 310 (Well TS-306)	The permeability of different partition blocks varies greatly, and some horizontal drainage wells exist
Tunlun	No. 3	P_1 (Shanxi Formation)	2.0–3.0	400–900	0.02–0.10	> 1100 (Tun well 2)	The permeability is generally low
Enhon	No. 9, 16, and 23	P_2 (Xuanwei Formation)	1.2–1.5	500–1500	0.04–6.10	500 (Well EH-5)	High porosity and permeability
Jixian–Hancheng	No. 5 and 8	C—P (Shanxi Formation, Taiyuan Formation)	1.1–2.1	350–1500	0.01–43	852 (Jishi well 3); > 2500 (Jishi well 1)	The permeability of the two layers of coal is very different, and some CBM wells allow the two layers of coal to be discharged together
Zaoyuan	No. 3	P_1 (Shanxi Formation)	0.5–0.8	550–750	0.5–1.8	706 (Well FZ-007)	The fracture has strong conductivity, and the permeability is very high
Baode	No. 8 and 9	C—P (Shanxi Formation, Taiyuan Formation)	0.8–1.4	400–800	0.01–3.73	1482 (Well 3V)	The coal reservoir has a high water content, and the permeability difference is enormous.
Binchang	No. 4	J_2 (Yanan Formation)	0.5–0.7	400–650	3.06–5.73	12964 (Well DFSC-02)	High permeability and porosity
Tiefa	No. 4–2, 9, 12, and 15–2	J_3—K_1 (Fuxin Formation)	0.5–0.6	300–950	0.10–1.60	5750 (Well DT3)	High gas content and permeability

permeability further. In the development of CBM, acidizing treatment is to inject one or several acid solutions (such as inorganic acid, organic acid, and multi-component acid) into the formation through the wellbore, and use the acid solution to dissolve the rock cement or the plugging material in the formation pores and fractures, thus becoming an effective way to improve the permeability of coal reservoir (Du et al., 2019). Since the adsorption capacity of coal for CO_2 is higher than that for CH_4, the permeability of coal reservoir can be improved by competitive adsorption (Du et al., 2019). The coal samples of medium and high-rank coal were collected from Tunliu and Shihe coal mine in China, respectively. Experimental apparatus adopting mixed gas displacement testing machine, Its working principle is that the stress loading device can apply confining and axial pressure and simulate the stress state of the coal sample, and the gas pipelines at both ends of the sample are respectively connected with a metering pump, flow rate controller, flow gauge, pressure gauge. The equipment can inject gas into coal samples at different pressures and collect corresponding data to calculate permeability (Fig. 14). The results show that the permeability of coal reservoir decreases first and then increases with the increase of gas injection pressure (Fig. 15). The higher the confining pressure is, the smaller the permeability of coal reservoir is. The permeability of medium rank coal samples is roughly equal when the gas injection pressure is 1.3 and 6.25 MPa. The permeability of high-rank coal samples is roughly equal when the gas injection pressure is 2.25 and 6.25 MPa. Besides, The effects of acoustic field can promote the diffusion of CBM and generally increase the permeability of coal reservoirs by more than 10%. There is a negative exponential relation between CBM flow increments and the source (Rice et al., 2008).

4 Petrophysics heterogeneity of CBM reservoir

4.1 Microscale petrophysics heterogeneity

The research on coal reservoir heterogeneity is mainly reflected in macroscopic and microscopic aspects (Zhang et al., 2018). Macro-heterogeneity is mainly studied from the three levels of inter-layer, in-layer, and plane. Micro-heterogeneity is mainly studied from the distribution law of pore structure, porosity, pore size distribution, fracture size, and structure (Li et al., 2016a). Figure 16 suggests that the 3D spatial distribution of the pore-fracture system has apparent heterogeneity. Besides, it can be clearly seen that X-ray μ-CT data have a larger number of pore-fractures than the FIB-SEM data. The research methods mainly include SPSS factor analysis, Lorentz curve, comprehensive gray evaluation based on GIS, heterogeneous degree coefficient, statistics, gray set pair analysis,

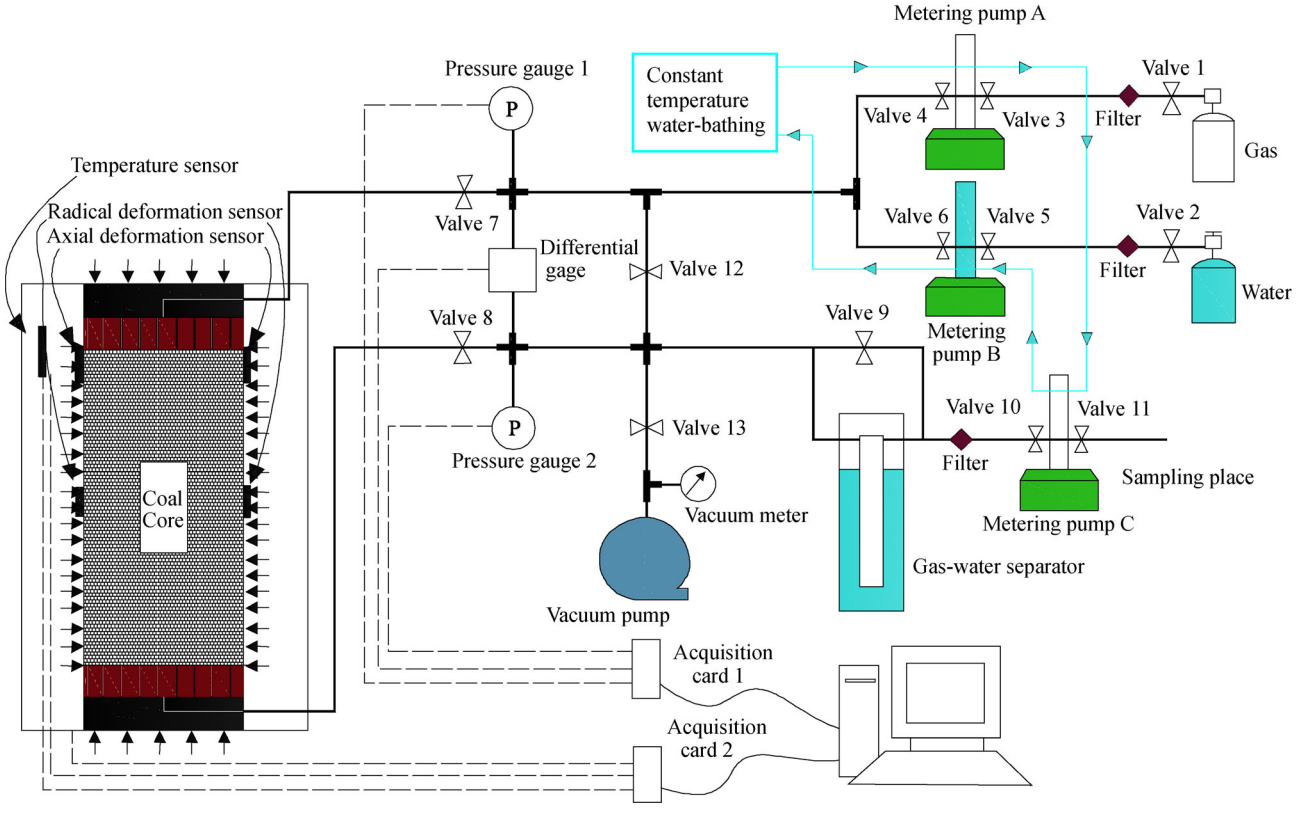

Fig. 14 Working principle of mixed gas displacement testing machine (Ni et al., 2018).

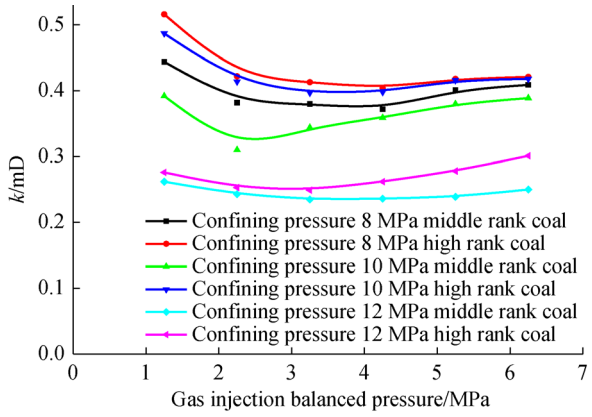

Fig. 15 Permeability change under different confining pressure and gas injection pressure.

X-ray diffraction, high-pressure mercury injection experimental analysis, and transmission electron microscopy (Prinz et al., 2004; Radlinski et al., 2004; Yao et al., 2009; Majdi et al., 2012; Yao and Liu, 2012).

The study of microscale petrophysics heterogeneity is active, mainly reflected in the distribution rules of porosity, pore size distribution, and mineral composition (Zhang et al., 2018). The study on the pore development characteristics of coal reservoirs in north China shows that both the porosity and pore size distribution are heterogeneous. Porosity was generally high, ranging from 2.38% to 10.3%, with an average of 5.72%. In particular, the average porosity of Jiaozuo and Yinggong coal fields is over 10%, which is rare in coal. The coal porosity of Anghe and Pingdingshan coal fields is also high, while other coal fields are generally low. Even in the same mining area, each sample's porosity varies greatly (Yao et al., 2010b). The pores of coal reservoir in north China are generally dominated by adsorption pores, accounting for about 80%, among which the small pores are the most developed, generally accounting for more than 50%. The seepage pores are generally undeveloped, among which the macropores are more developed than the mesopores. From the perspective of the output contribution to CBM, the coal pore structure in Jiaozuo and Huaibei coal fields is the best, with a large number of micropores and small pores as well as a certain proportion of mesopores and macropores, which is conducive to the desorption, seepage, and production of gas. In the Anhe, Yinggong, Huainan, and Pingdingshan coalfield, the pores of all levels are more evenly developed, which is also conducive to the storage and production of CBM (Yao et al., 2010a). The proportion of micropores and small pores is large so that the CBM can be produced successfully by means of exogenous fractures in northern, central, and southern Qinshui Basin. However, the proportion of micropores and small pores in Yongxia and Datong coal fields is too large, which is not conducive to the production of CBM (Table 2). The distribution and quantity of pores in mineral components vary significantly at the microscale. Many clay minerals, berry-shaped pyrite, granular pyrite, brittle quartz particles, and organic matter particles are scattered and disordered. The pores in them are difficult to observe under the horizon of 100 μm. Some slip-shaped clay minerals, silty quartz particles, organic particles, and pyrite crystals are stacked closely together, and a small number of pores can be observed under the horizon of 10 μm.

4.2 Macroscale petrophysics heterogeneity

Coal reservoirs are affected by sedimentary environment, metamorphism, diagenesis, and tectonic movements. There are generally uneven changes in in-plane distribution and longitudinal space (Ahmad et al., 2019; Li et al., 2020b). The heterogeneity of coal seam formed by fluvial peat bogs was the strongest, followed by that formed by delta peat bogs, and the heterogeneity of coal seam formed by peat flat was the weakest (Scott, 2002). In the same coal seam, the gas-bearing heterogeneity of the coal reservoir is shown as "the heterogeneity of the longitudinal top and bottom is weak, and that of the middle is strong. The heterogeneity near or across the fault area is strong, while the heterogeneity in the simple structure area is weak" (Mazumder et al., 2012). The heterogeneity of fracture density development in coal reservoir is characterized by "both the fractal dimension and the stagger coefficient of the fault zone are generally vast, and the heterogeneity is strong." The permeability heterogeneity of coal reservoir is characterized by "vertical distribution of coal with different metamorphic degrees, more internal fractures in the middle than in the bottom, serious permeability stratification and significant heterogeneity" (Kumar et al., 2016; Lupton et al., 2020). The development of natural fractures in adjacent CBM Wells reservoirs in the same block may also vary greatly. The microseismic monitoring results show that the fracture extension directions of CBM well SZ1 in the Shizhuang block of Qinshui Basin are 48°NE and 50°NW (Fig. 17(a)), while the fracture extension directions of adjacent CBM well SZ2 are 51°NE (Fig. 17(b)). Affected by tectonic movement, the original structure of the coal reservoir changes, and the heterogeneity becomes more potent with the structural deformation and the enhancement of the stress field (Karacan and Okandan, 2000; Fan et al., 2010). Different pore configuration, fracture distribution, and seepage networks were formed in the multi-stage tectonic movement and different coal-forming environments, which resulted in a precise correlation between the coal reservoir heterogeneity and the degree of CBM exploitation (Fan et al., 2010;).

In general, the phenomenon of coal reservoir height heterogeneity is widespread in China. The exploration and

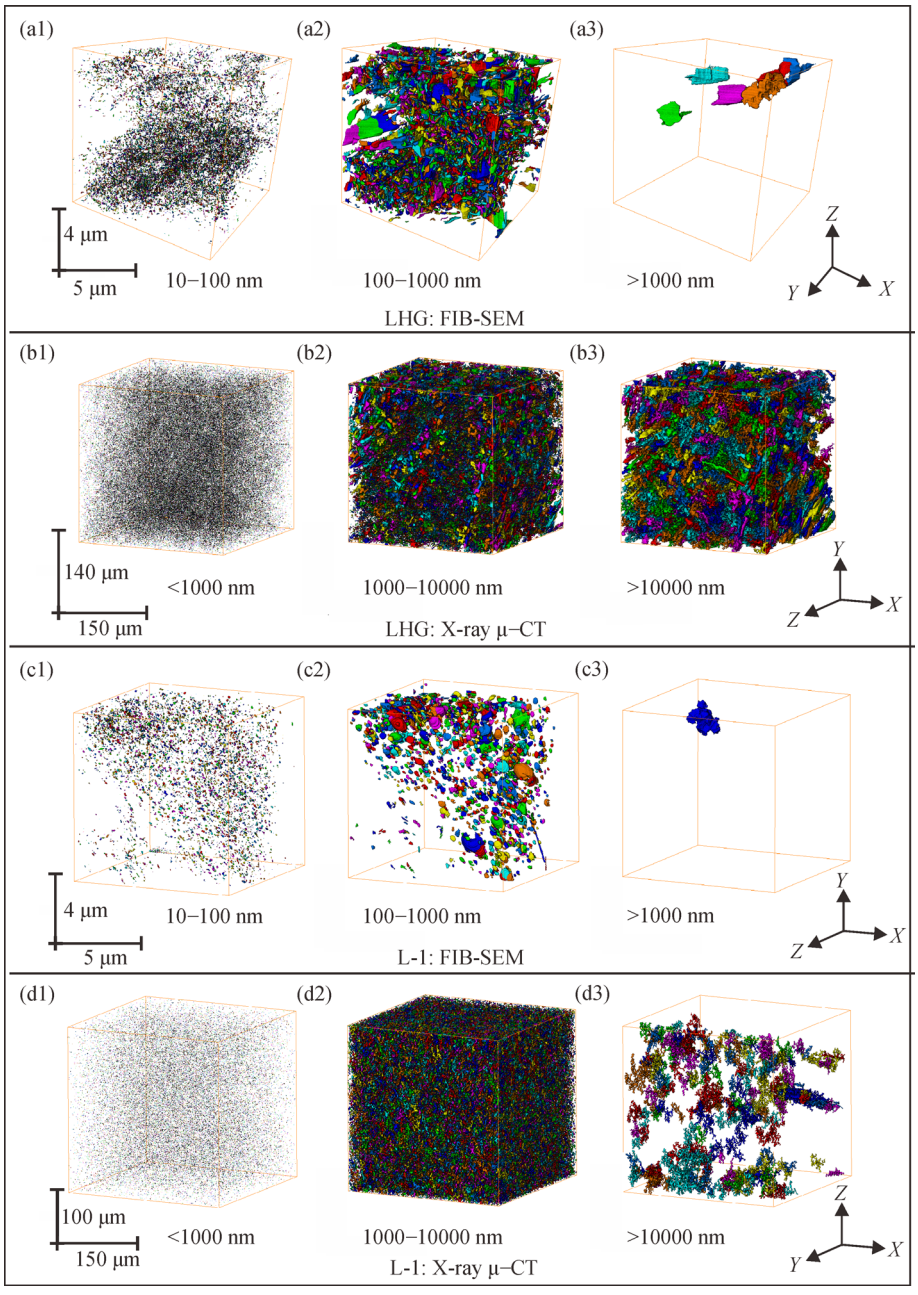

Fig. 16 3D spatial distribution of pore-fraction system in different ranges. a1–a3: FIB-SEM data of sample LHG; b1–b3: X-ray μ–CT data of sample LHG; c1-c3: FIB-SEM data of sample L-1; d1–d3: X-ray μ–CT data of sample L-1 (Li et al., 2020b).

development of CBM will pay more attention to the distribution of reservoir heterogeneity. There are many kinds of research on the corporality parameters of coal porosity, pore structure, coal quality, vitrinite reflectance, and industrial components. The study on lithology heterogeneity of deep low-rank coal, especially the large dip angle reservoirs, needs to be further revealed. Besides, the control mechanism of reservoir heterogeneity from the geological structure and coal-forming environment needs to be further explored for the coal reservoir with high H_2S concentration.

5 Geological controls on CBM reservoir petrophysics

5.1 Geological stress

Geological stress refers to the stress state in the earth's crust. Both the paleotectonic stress and the present stress control the permeability of coal seam (Ni et al., 2019). There are cleat systems with different degrees of development in coal seams (Cai et al., 2019). The opening degree of the cleat is greatly influenced by the geological stress

Table 2 Pore development and pore size distribution of coal reservoir in north China

Coalfield (Basin)	Mercury injection test data					Pore size distribution			
	Porosity /%	Displacement pressure/MPa	The average diameter of pore throat /μm	Incoming mercury saturation/%	The efficiency of mercury withdrawal /%	Macropores /%	Mesopores /%	Small pores /%	Micropores /%
Northern Qinshui	3.50	7.01	0.06	23.1	65.6	6.5	6	67.0	20.5
Central Qinshui	3.78	6.83	0.05	19.4	61.0	7.4	6.1	69.3	17.2
Southern Qinshui	4.23	7.67	0.12	24.6	65.6	8	7.9	26.4	57.7
Datong	4.24	11.37	0.04	22.0	82.7	4.3	2.6	32.4	60.7
Pingdingshan	6.75	7.93	0.08	43.4	73.0	9.1	10.3	54.7	25.9
Anhe	8.38	3.71	0.18	27.5	43.7	11.4	12.2	71.4	5
Jiaozuo	10.30	3.98	1.26	36.9	39.5	20.7	11	37.7	30.6
Yongxia	2.80	7.08	0.04	17.3	65.7	6	5.7	49.1	39.2
Xinggong	10.38	3.92	0.23	31.8	55.8	13.8	11.1	59.8	15.3
Huainan	4.61	0.07	12.27	37.1	33.1	18.8	6.5	57.9	16.8
Huaibei	3.94	0.15	11.14	55.2	37.8	27.6	15.4	37.7	19.3

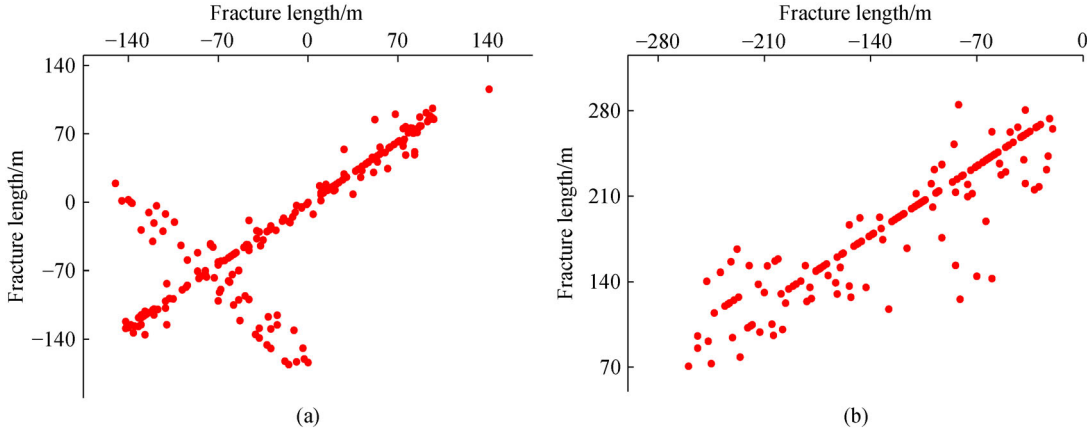

Fig. 17 Microseismic monitoring results of CBM well. (a) well SZ1; (b) well SZ2 (Jia et al., 2019).

field. The change of geological stress field can cause the cleat opening and closing, affecting the change of coal seam permeability. All the stresses in the untapped coal reservoir are in equilibrium. The pressure of coal reservoir gradually decreases with the drainage of water and gas, increasing effective stress of coal reservoir, the compression and closure of pore-fracture in coal reservoir, and the significant elastoplastic deformation of coal body in the process of CBM development, which leads to the apparent decrease of permeability.

The geological stress is closely related to the mechanical parameters of coal petrography. It can accumulate coal bed stress under the conditions of rock integrity and high elasticity modulus (Jiang et al., 2016). The elasticity and mechanical strength of coal decrease with the increase of temperature, while the plasticity increases. The effect of temperature on the mechanical properties of coal is so small that the effect on the overall mechanical strength of coal can be ignored. The elastic properties and mechanical strength of coal are different in different stress ranges. The elastic modulus of coal increases with the increase of effective confining pressure, while Poisson's ratio decreases in the elastic deformation stage. When plastic deformation occurs, the corresponding stress and strain value increase with the increase of effective confining pressure, and the yield point becomes more evident in the plastic deformation stage. The residual strength of coal also increases with effective confining pressure in the residual strength stage. Due to the differences in macerals, metamorphism degree, and lithology of the roof, the mechanical properties of coal rock and surrounding rock are quite different, resulting in different geological stress

values accumulated by different lithotypes. Different lithotypes have apparent differences in petrophysical properties, which may lead to different directions of geological stress. At the same time, lithotypes are affected by tectonism. The heterogeneity of geological stress also has a significant influence on the late coal petrography reconstruction.

There are many methods to measure geological stress, such as field monitoring, microseismic, laboratory testing, based on deformation or related physical quantities to obtain the state of geological stress, which belongs to indirect measurement. In comparison, the hydraulic fracturing method can measure the relatively reliable geological stress, which can be regarded as the direct measurement of geological stress within a certain accuracy range (Ni et al., 2019). Its calculation method shows in Eq. (3).

$$\begin{cases} \sigma_{\mathrm{H}} = 3\sigma_{\mathrm{h}} - p_{\mathrm{f}} - p_0 + s_{\mathrm{t}} \\ \sigma_{\mathrm{h}} = p_{\mathrm{ISTP}} \end{cases}, \tag{3}$$

where σ_{H} is the maximum horizontal principal stress, MPa; σ_{h} denotes the minimum horizontal principal stress, MPa; p_0 is the coal reservoir pressure, MPa; p_{f} is the pressure on the coal to be fractured, MPa; s_{t} denotes the tensile strength of the coal, MPa; p_{ISTP} can be read directly from the hydraulic fracturing curve.

When the hydraulic fracturing curve is standard, the method of hydraulic fracturing is more accurate to obtain geological stress. However, the fracture pressure will be higher than the actual value when the drilling results in the expansion of well diameter or pollution near the well are caused by cementing. Besides, the unreasonable pumping procedure in the fracturing process may increase in the construction pressure, resulting in the instantaneous shut-in pressure is inconsistent with the actual situation. At this time, the acoustic logging method can obtain accurate geological stress (Eq. 4).

$$\begin{cases} \sigma_{\mathrm{H}} = \left(\dfrac{\mu}{1-\mu} + A\right)(\sigma_{\mathrm{v}} - \varphi p_0) + \varphi p_0 \\ \sigma_{\mathrm{h}} = \left(\dfrac{\mu}{1-\mu} + B\right)(\sigma_{\mathrm{v}} - \varphi p_0) + \varphi p_0 \end{cases}, \tag{4}$$

where μ is the Poisson's ratio of the coal; σ_{v} is vertical stress, MPa; A and B are the tectonic stress coefficients; φ is the pressure contribution coefficient of the coal reservoir.

Given that:

$$\varphi = 1 - \frac{\rho\,(\,3V_{\mathrm{p}}^2 - 4V_{\mathrm{s}}^2\,)}{\rho_{\mathrm{m}}\,(\,3V_{\mathrm{mp}}^2 - 4V_{\mathrm{ms}}^2\,)}, \tag{5}$$

where ρ is the bulk density of coal, g/cm^3; ρ_{m} is the skeletal density of coal, g/cm^3; V_{mp} and V_{ms} are the longitudinal and transverse velocities of the skeleton, m/s; V_{p} and V_{s} are vertical and transverse wave velocities respectively, m/s.

5.2 Sedimentary environment

The thickness and distribution areas of coal are mainly controlled by the sedimentary environment (Karayiğit et al., 2018; Eble et al., 2019). The No. 3 coal seam of Shanxi Formation developing in delta-lake facies has a large thickness and stable distribution, while the No. 15 coal seam of Taiyuan Formation developing in coastal shelf and lagoon is relatively thin and unstable. Whether in tidal flat, delta, or flood basin of the river system, the coal seam with significant thickness and stable distribution can only be formed if the sedimentation rate is the same as the deposition rate. On the contrary, the relatively volatile environment is difficult to form a stable distribution of coal seams (Zhao et al., 2018). The sedimentary environment has a direct influence on the content of coal components, and the content of vitrinite is high in the coal seam formed in the water-covered and reducing environment (Goodarzi et al., 2019). The more reductive the environment is, the higher the content of telocollinite is, the more developed the cleat is, and the better the permeability is. The No. 3 coal seam of Shanxi Formation formed in the front margin of the delta, which is easy to form the overlying water swamp facies with substantial reducing property, more gelatinous microcomponent, and better reservoir permeability in this environment. The No. 15 coal seam of Taiyuan Formation was formed in a peat marsh. Due to the high content of sulfur in the coal affected by the transgression, the coal seam has a strong reducing property.

The intense and frequent evolutions of coal facies in the coal-accumulation basin lead to the different development of coal reservoirs both horizontally and longitudinally, which leads to the formation of substantial reservoir heterogeneity (Oskay et al., 2019). Most of the coal reservoirs in the Ordos Basin formed in forest peat marsh, and living water peat marsh facies have useful properties, while the coal reservoirs formed in dry peat marsh facies have medium or weak properties. The sedimentary environment affects both mineral composition and ash content (Chinelatto et al., 2020). Some of the pores are filled with minerals due to mineralization, which leads to a decrease in reservoir permeability. This phenomenon is common in north China. Ash contents are mainly inorganic, most of which are derived from terrigenous detritus and transgression. Generally, the higher the ash yield is, the higher the mineral content of the reservoir is. Besides, there is a linear relationship between the ash content and the fractal dimension of coal reservoir pore structure. Most of the coal micropores in northern Qinshui Basin are filled with ash due to frequent sedimentation, resulting in a high fractal dimension and substantial heterogeneity of pore structure.

5.3 Coal petrology and composition

The petrological characteristics of coal reservoir can directly reflect the genesis of coal seam and the difficulty degree of coal powder production, mainly through controlling permeability, adsorption-desorption characteristics, and gas-bearing to affect gas-water migration. An in-depth study of macroscopic coal rocks, microscopic coal rocks, macerals, and coal facies can enrich the geological theory of CBM and guide the rational and efficient development of CBM resources (Ibrahim and Nasr-El-Din, 2015; Oskay et al., 2019).

The microscopic coal rocks and macerals control the development of microfractures. The difference of maceral in transverse and vertical direction leads to the anisotropic heterogeneity of microfracture development (Eble et al., 2019). The microfractures develop more and more with the increase of the brightness of coal. The micromirror coal content has a significant positive correlation with microfractures' development (Yao et al., 2010a; Karayiğit et al., 2018). Different macerals of coal have vast differences in gas generation potential and adsorption capacity. The exinite has the most considerable gas generation potential, followed by the vitrinite and inertinite. The vitrinite has the largest adsorption capacity, followed by the inertinite and exinite (Yao et al., 2010a; Li et al., 2017a). The content of the vitrinite at the density level of −1.35 g/cm^3 increased first and then decreased with the increase of the grinding time by analyzing the macerals of low-rank bituminous in Shigetai coal mine. The inertinite content at the density level from 1.35 to 1.40 g/cm^3 showed a similar trend (Table 3). The reason is that both the vitrinite and inertinite dissociate better in the early stage of grinding. The dissociation degree between the inertinite and the minerals increases with the increase of the grinding time, which leads to the tendency that both the vitrinite and inertinite increase first and then decrease at different density levels (Radlinski et al., 2004). In the case of coal with higher inertinite and lower vitrinite, the inertinite plays a leading role in controlling the porosity. The coal metamorphic degree and porosity change regularly when the inertinite is lower, and the vitrinite is higher (Crosdale et al, 1998). The macerals of coal dominate the uneven distribution of permeability and porosity, while coal facies control it. Through the reflection of the frequent changes of plant types, preservation conditions, water flow types, and overburden depth, the coal facies dominates the macerals, which affects the degree of fracture development and permeability, and indirectly causes the change of coal reservoir pressure, ultimately leading to the formation of substantial reservoir heterogeneity (Zhang et al., 2009; Li et al., 2017b). There is an apparent relationship between coal facies and pore development. As the value of tissue preservation index (TPI) and wood index (WI) increased, the percentage of micropores and transition pores ($< 10^2$ nm) increased. The negative correlation between TPI or WI and macropores could be observed, while there was no significant correlation between pore size between 10^2 nm and coal facies index, pore size between 10^3 nm and coal facies index (Fig. 18). Figure 19 shows the correlation analysis between groundwater index (GWI) and various types (Type A, B, C, and D) of fractures for coal samples. For type A and type B fractures, which are slightly developed in the coal samples with a range from 0 to 2 and 0 to 3 per 9cm^2, respectively, these two types of fractures do not have any trend with the GWI. Fracture frequency of Type C and Type D shows a positive relationship as GWI increases, as shown in Figs. 19(c) and 19(d). There is a comprehensive elastic self-regulating effect in coal petrography, which largely counteracts the destructive effect of unfavorable geological conditions on the gas reservoir (Lu et al., 2020). The elastic self-regulation effect of coal petrography is negatively correlated with coal rank under the same pressure of the CBM system, which is strictly controlled by the evolution of coal structure with the change of coal rank (Davudov and Moghanloo, 2018). No matter what the coal rank is, the mechanical properties of coal petrography are mainly controlled by stress. As the

Table 3 The macerals of coal samples with different grinding rod time (Tao et al., 2020)

Grinding rod time/min	Macerals	Density level/(g·cm^{-3})		
		< 1.35	1.35–1.40	> 1.40
5	Vitrinite	73.26%	34.57%	49.77%
	Inertinite	26.74%	65.43%	50.23%
10	Vitrinite	75.83%	31.84%	44.62%
	Inertinite	24.17%	68.16%	55.38%
15	Vitrinite	74.49%	32.80%	45.11%
	Inertinite	29.51%	67.20%	54.89%
20	Vitrinite	70.78%	34.70%	45.99%
	inertinite	34.22%	65.30%	54.01%
30	Vitrinite	66.53%	39.77%	46.45%
	Inertinite	33.47%	60.23%	53.55%

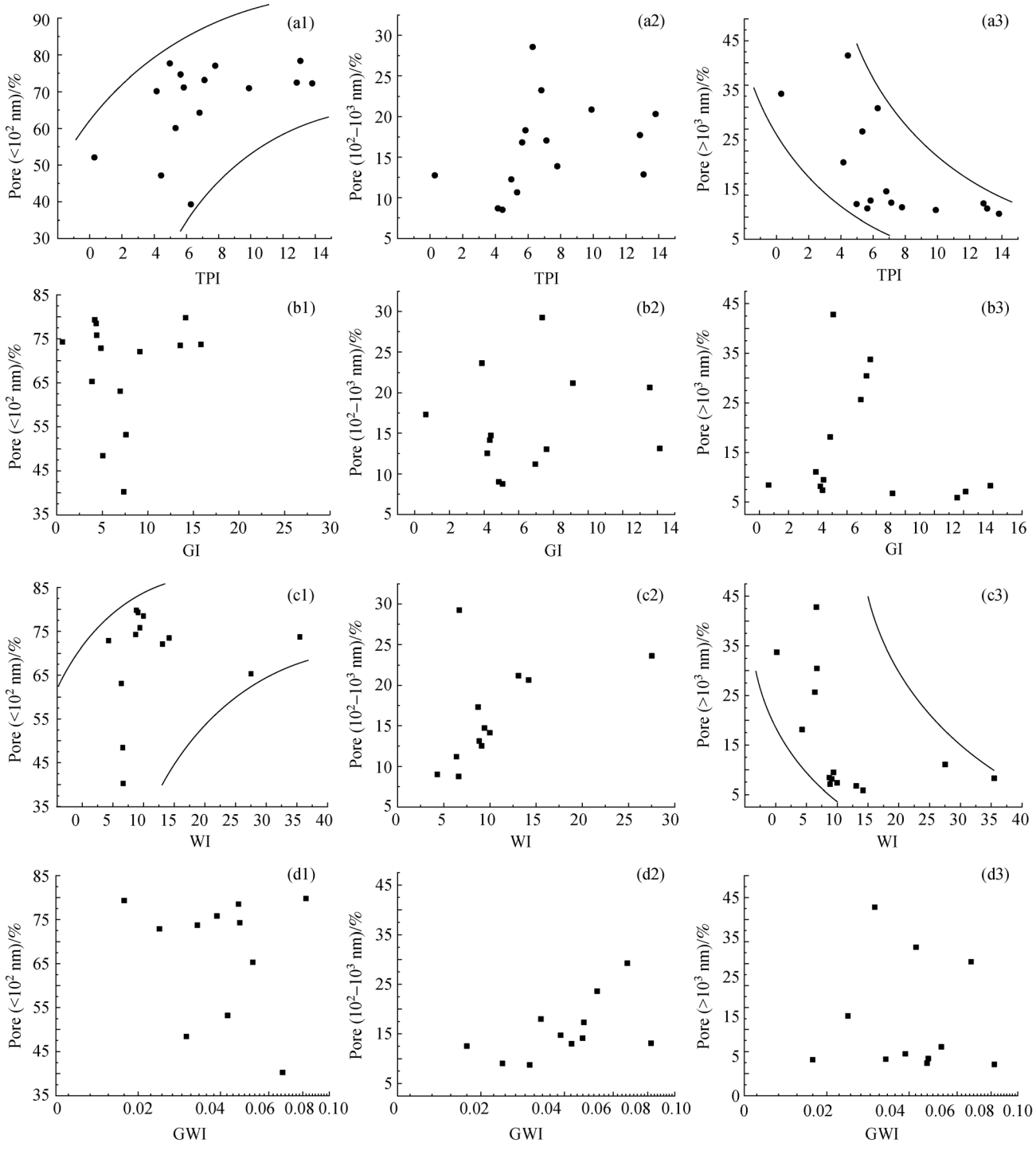

Fig. 18 Relationships between the pore size and coal facies index. (a1) the relationship between pore size ($< 10^2$ nm) and TPI; (a2) the relationship between pore size (10^2–10^3 nm) and TPI; (a3) the relationship between pore size ($> 10^3$ nm) and TPI; (b1) the relationship between pore size ($< 10^2$ nm) and gelification index (GI); (b2) the relationship between pore size (10^2–10^3 nm) and GI; (b3) the relationship between pore size ($> 10^3$ nm) and GI; (c1) the relationship between pore size ($< 10^2$ nm) and WI; (c2) the relationship between pore size (10^2–10^3 nm) and WI; (c3) the relationship between pore size ($> 10^3$ nm) and WI; (d1) the relationship between pore size ($< 10^2$ nm) and groundwater index (GWI); (d2) the relationship between pore size (10^2–10^3 nm) and GWI; (d3) the relationship between pore size ($> 10^3$ nm) and GWI (Lu et al., 2020).

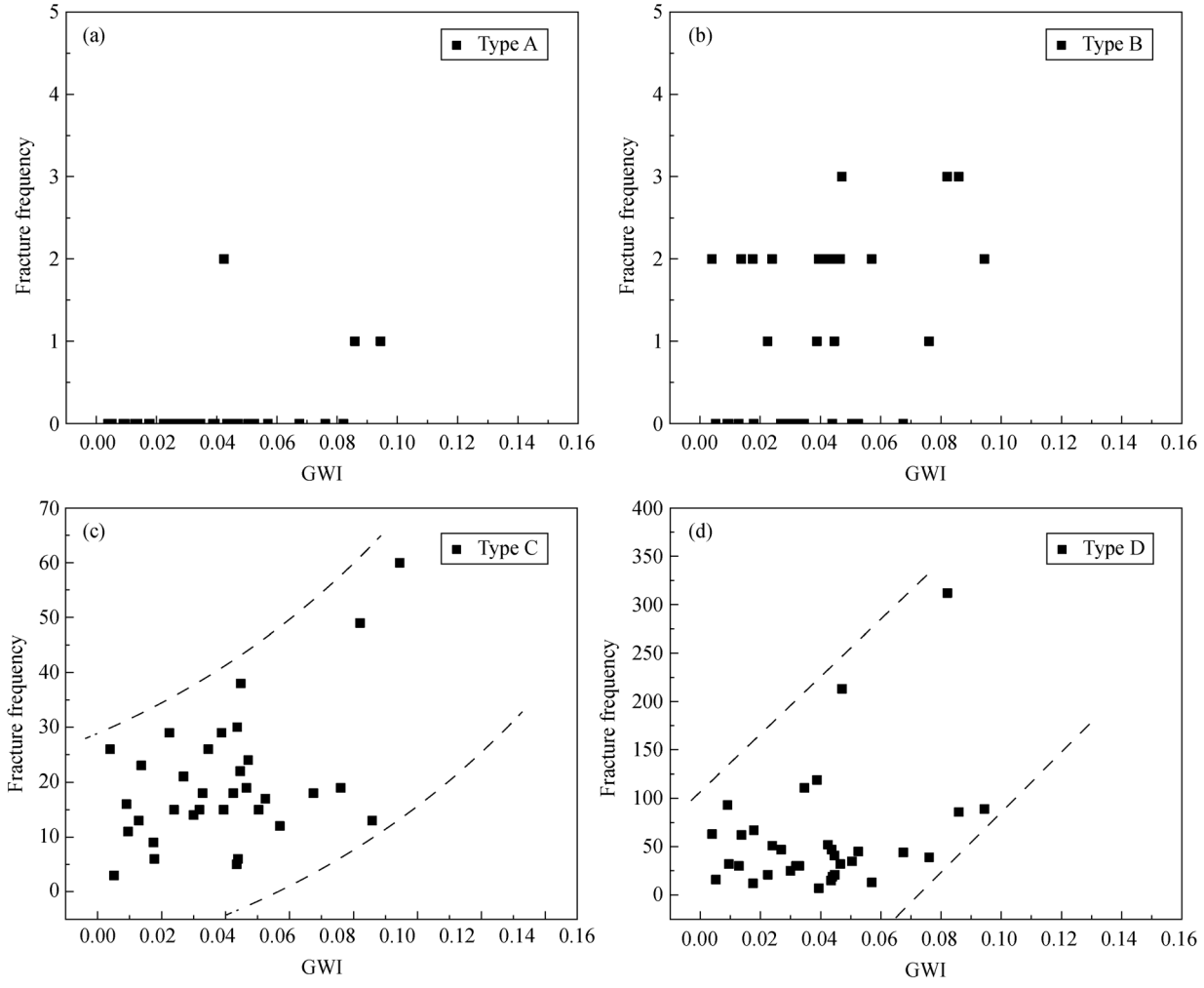

Fig. 19 Relationships between the microfractures and GWI. (a) GWI against type A fractures; (b) GWI against type B fractures; (c) GWI against type C fractures; (d) GWI against type D fractures (Lu et al., 2020).

stress increases, the opening degree of pore-fracture decreases, the mechanical strength of coal petrography increases first and then decreases, and the elastic modulus also increases first and then decreases (Mora and Wattenbarger, 2009). The strength of coal petrography is influenced by the coupling action of temperature and pressure. The influence of temperature is more critical than the confining pressure in the low strain stage of medium and high- rank coals, while the confining pressure plays a leading role in the strength of coal petrography in the high strain stage.

In a word, previous research on coal petrology characteristics, macerals, and coal facies has achieved fruitful results, promoting the effective reformation of shallow coal reservoirs and avoiding the contradictions caused by the heterogeneity of some reservoirs in the process of drainage. However, facing the real situation of shallow CBM shortage, the spatial multi-layer production, the storage-seepage characteristics of deep CBM dominated by coal petrology, and the coupling relationship of the optimized productivity should be further revealed to promote the maturation of reservoir engineering theory.

6 Conclusions

This paper summarizes the research progress of petrophysics characteristics from the aspects of pore-fracture evolution, permeability, heterogeneity, and geological controls. Three characterization methods of pore-fracture and the evolution characteristics of multiscale pore-fractures are introduced in detail. The non-fluid injection method has broad development prospects. The systematic rule of permeability change is analyzed, and then the corporality characters under the restriction of coal petrology are clarified. On this basis, the leading direction of petrophysics characteristics in CBM reservoirs is prospectively proposed. The following conclusions can be made:

1) The characterization of pore-fracture has gone

through three stages: qualitative and semiquantitative evaluation of pore-fracture by various techniques, quantitatively refined characterization of pore-fracture by integrating multiple methods including nuclear magnetic resonance analysis, liquid nitrogen, and mercury intrusion, and advanced quantitative characterization methods of pore-fracture by high-precision experimental instruments (focused-ion beam-scanning electron microscopy, small-angle neutron scattering and computed tomography scanner) and testing methods (μ-CT scanning and X-ray diffraction), which significantly promoted the development of the pore-fracture research.

2) Tectonic stress is the most crucial factor determining the permeability, but there are vast differences in the impact on shallow and deep coal seams. The effects of acoustic field can promote the diffusion of CBM and generally increase the permeability of coal reservoirs by more than 10%. The heterogeneity of CBM reservoirs increases with the enhancement of the tectonic deformation and stress field, and there is a precise correlation between the heterogeneity of coal reservoir and the degree of CBM exploitation.

3) The study on lithology heterogeneity of deep low-rank coal, especially the high-dip angle reservoirs, needs to be further revealed. Facing the real situation of shallow CBM shortage, the spatial multi-layer production, the storage-seepage characteristics of deep CBM dominated by coal petrology, and the coupling relationship of the optimized productivity should be further revealed to promote the maturation of CBM reservoir engineering theory.

Acknowledgements This research was funded by the National Natural Science Foundation of China (Grant Nos. 41830427, 41772160 and 41922016). We are very grateful to the reviewers and editors for their valuable comments and suggestions.

References

Ahmad M, Ahmed N, Khalid P, Badar M A, Akram S, Hussain M, Anwar M A, Mahmood A, Ali S, Rehman A U (2019). Impact of pore fluid heterogeneities on angle-dependent reflectivity in poroelastic layers: a study driven by seismic petrophysics. Geomech Eng, 17: 343–354

Akhondzadeh H, Keshavarz A, Al-Yaseri A Z, Ali M, Awan F U R, Wang X, Yang Y F, Iglauer S, Lebedev M (2020). Pore-scale analysis of coal cleat network evolution through liquid nitrogen treatment: a Micro-Computed Tomography investigation. Int J Coal Geol, 219: 103370

Cai J C, Sun S Y, Habibi A, Zhang Z E (2019). Emerging advances in petrophysics: porous media characterization and modeling of multi-phase flow. Energies, 12(2): 282

Cai Y D, Liu D M, Pan Z J, Yao Y B, Li J Q, Qiu Y K (2013). Pore structure and its impact on CH_4 adsorption capacity and flow capability of bituminous and subbituminous coals from northeast China. Fuel, 103: 258–268

Cai Y D, Liu D M, Mathew J P, Pan Z J, Elsworth D, Yao Y B, Li J Q, Guo X Q (2014). Permeability evolution in fractured coal-Combining triaxial confinement with X-ray computed tomography, acoustic emission and ultrasonic techniques. Int J Coal Geol, 122: 91–104

Cai Y D, Li Q, Liu D M, Zhou Y F, Lv D W (2018). Insights into matrix compressibility of coals by mercury intrusion porosimetry and N_2 adsorption. Int J Coal Geol, 200: 199–212

Chinelatto G F, Belila A M, Basso M, Souza J P, Vidal A C (2020). A taphofacies interpretation of shell concentrations and their relationship with petrophysics: a case study of Barremian-Aptian coquinas in the Itapema Formation, Santos Basin-Brazil. Mar Pet Geol, 116: 104317

Clarkson C R, Qanbari F (2016). A semi-analytical method for forecasting wells completed in low permeability, undersaturated CBM reservoirs. J Nat Gas Sci Eng, 30: 19–27

Crosdale P J, Beamish B B, Valix M (1998). Coalbed methane sorption related to coal composition. Int J Coal Geol, 35(1–4): 147–158

Davudov D, Moghanloo R G (2018). Impact of pore compressibility and connectivity loss on shale permeability. Int J Coal Geol, 187: 98–113

Du Y, Sang S X, Pan Z J, Wang W F, Liu S Q, Fu C Q, Zhao Y C, Zhang J Y (2019). Experimental study of supercritical CO_2-H_2O-coal interactions and the effect on coal permeability. Fuel, 253: 369–382

Eble C F, Greb S F, Williams D A, Hower J C, O'Keefe J M K (2019). Palynology, organic petrology and geochemistry of the Bell coal bed in Western Kentucky, Eastern Interior (Illinois) Basin, USA. Int J Coal Geol, 213: 103264

Fan J J, Ju Y W, Hou Q L, Tan J Q, Wei M M (2010). Pore structure characteristics of different metamorphic-deformed coal reservoirs and its restriction on recovery of coalbed methane. Earth Sci Front, 17(5): 325–335

Fang X L, Cai Y D, Liu D M, Zhou Y F (2018). A mercury intrusion porosimetry method for methane diffusivity and permeability evaluation in coals: a comparative analysis. Appl Sci (Basel), 8(6): 860–876

Fu X H, Qin Y, Zhang W H, Wei C T, Zhou R F (2005). Fractal classification and natural classification of coal pore structure based on migration of coal bed methane. Chin Sci Bull, 66(S1): 51–55

Goodarzi F, Haeri-Ardakani O, Gentzis T, Pedersen P K (2019). Organic petrology and geochemistry of Tournaisian-age Albert Formation oil shales, New Brunswick, Canada. Int J Coal Geol, 205: 43–57

Guo H Y, Su X B, Xia D P, Ni X M, Li G S (2010). Relationship of the permeability and geological strength index (GSI) of coal reservoir and its significance. J China Coal Soc, 35(8): 1319–1322

Guo W, Yao Y B, Liu D M, Sun X X, Gao Y W (2016). Research on measurement of pores in coals with NMRC technique. Oil Gas Geol, 7(1): 141–148

Harpalani S, Chen G (1995). Estimation of changes in fracture porosity of coal with gas emission. Fuel, 74(10): 1491–1498

Hodot B B (1966). Outburst of Coal and Coalbed Gas. Beijing: China Industry Press (in Chinese)

Hoffman B T, Caers J (2005). Regional probability perturbations for history matching. J Petrol Sci Eng, 46(1–2): 53–71

Hou S H, Wang X M, Wang X J, Yuan Y D, Pan S D, Wang X M (2017). Pore structure characterization of low volatile bituminous coals with different particle size and tectonic deformation using low pressure

gas adsorption. Int J Coal Geol, 183: 1–13

Ibrahim A F, Nasr-El-Din H A (2015). A comprehensive model to history match and predict gas/water production from coal seams. Int J Coal Geol, 146: 79–90

IUPAC (1972). Manual of symbols and terminology. Pure Appl Chem, 31: 578

Jia Q F, Ni X M, Zhao Y C, Cao Y X (2019). Fracture extension law of hydraulic fracture in coal with different structure. Coal Geol Explor, 47(2): 51–57

Jiang B, Qu Z H, Wang G G X, Li M (2010). Effects of structural deformation on formation of coalbed methane reservoirs in Huaibei coalfield, China. Int J Coal Geol, 82(3-4): 175–183

Jiang B, Wang J L, Qu Z H, Li C G, Wang L L, Li M, Liu J G (2016). The stress characteristics of the Daning-Jixian Area and its influence on the permeability of the coal reservoir. Earth Sci Front, 23(3): 17–23

Jiang W P, Song X Z, Zhong L W (2011). Research on the pore properties of different coal body structure coals and the effects on gas outburst based on the low-temperature nitrogen adsorption method. J China Coal Soc, 36(4): 609–614

Ju Y W, Jian B, Hou Q L, Wang G L, Fang A M (2005). Structural evolution of nano-scale pores of tectonic coals in southern north China and its mechanism. Acta Geol Sin, 79(2): 269–285

Karacan C Ö, Okandan E (2000). Fracture/cleat analysis of coals from Zonguldak Basin (northwestern Turkey) relative to the potential of coalbed methane production. Int J Coal Geol, 44(2): 109–125

Karacan C Ö (2013). Production history matching to determine reservoir properties of important coal groups in the Upper Pottsville formation, Brookwood and Oak Grove fields, Black Warrior Basin, Alabama. J Nat Gas Sci Eng, 10: 51–67

Karayiğit A IMastalerz M, Oskay R G, Buzkan I (2018). Bituminous coal seams from underground mines in the Zonguldak Basin (NW Turkey): insights from mineralogy, coal petrography, Rock-Eval pyrolysis, and meso- and microporosity. Int J Coal Geol, 199: 91–112

Kumar H, Elsworth D, Mathews J P, Marone C (2016). Permeability evolution in sorbing media: analogies between organic-rich shale and coal. Geofluids, 16(1): 43–55

Li J Q, Lu S F, Xue H T, Wang W M, Zhang P (2016a). Intra-stratal heterogeneity of high rank coalbed methane reservoirs and their quantitative evaluation: a case study from Zhengzhuang block in the southern Qinshui Basin. Oil Gas Geol, 37(1): 72–79

Li J Q, Zhang P F, Lu S F, Chen C, Xue H T, Wang S Y, Li W B (2019a). Scale-dependent nature of porosity and pore size distribution in lacustrine shales: an investigation by BIB-SEM and X-Ray CT Methods. J Earth Sci, 30(4): 823–833

Li J Q, Lu S F, Zhang P F, Cai J C, Li W B, Wang S Y, Feng W J (2020a). Estimation of gas-in-place content in coal and shale reservoirs: a process analysis method and its preliminary application. Fuel, 259: 116266

Li Q, Liu D M, Cai Y D, Zhao B, Qiu Y K, Zhou Y F (2020b). Scale-span pore structure heterogeneity of high volatile bituminous coal and anthracite by FIB-SEM and X-ray μ-CT. J Nat Gas Sci Eng, 81: 103443

Li Y, Tang D Z, Elsworth D, Xu H (2014). Characterization of coalbed methane reservoirs at multiple length scales: a cross-section from southeastern Ordos Basin, China. Energy Fuels, 28(9): 5587–5595

Li Y, Cao D Y, Wu P, Nin X L, Zhang Y (2017a). Variation in maceral composition and gas content with vitrinite reflectance in bituminous coal of the eastern Ordos Basin, China. J Petrol Sci Eng, 149: 114–125

Li Y, Zhang C, Tang D Z, Gan Q, Niu X L, Wang K, Shen R Y (2017b). Coal pore size distributions controlled by the coalification process: an experimental study of coals from the Junggar, Ordos and Qinshui Basins in China. Fuel, 206: 352–363

Li Y, Wang Z S, Pan Z J, Niu X L, Yu Y, Meng S Z (2019b). Pore structure and its fractal dimensions of transitional shale: a cross-section from east margin of the Ordos Basin, China. Fuel, 241: 417–431

Li Y, Yang J H, Pan Z J, Tong W S (2020c). Nanoscale pore structure and mechanical property analysis of coal: an insight combining AFM and SEM images. Fuel, 260: 116352

Li S, Tang D Z, Xu H, Tao S (2016b). Progress in geological researches on the deep coalbed methane reservoirs. Earth Sci Front, 23(3): 10–16

Li Z T, Liu D M, Cai Y D, Yao Y B, Wang H (2015). Pore structure and compressibility of coal matrix with elevated temperatures by mercury intrusion porosimetry. Energ Explor Exploit, 33(6): 809–826

Li Z T, Liu D M, Cai Y D, Ranjith P G, Yao Y B (2017c). Multi-scale quantitative characterization of 3-D pore-fracture networks in bituminous and anthracite coals using FIB-SEM tomography and X-ray μ-CT. Fuel, 209: 43–53

Liu S, Ma J, Sang S, Wang T, Du Y, Fang H (2018a). The effects of supercritical CO_2 on mesopore and macropore structure in bituminous and anthracite coal. Fuel, 223: 32–43

Liu Z S, Liu D M, Cai Y D, Pan Z J (2018b). The impacts of flow velocity on permeability and porosity of coals by core flooding and nuclear magnetic resonance: implications for coalbed methane production. J Petrol Sci Eng, 171: 938–950

Lu Y J, Liu D M, Cai Y D, Li Q, Jia Q F (2020). Pore-fractures of coalbed methane reservoir restricted by coal facies in Sangjiang-Muling coal-bearing Basins, northeast China. Energies, 13(5): 1196–1218

Lupton N, Connell L D, Heryanto D, Sander R, Camilleri M, Down D I, Pan Z J (2020). Enhancing biogenic methane generation in coalbed methane reservoirs—core flooding experiments on coals at *in situ* conditions. Int J Coal Geol, 219: 103377

Majdi A, Hassani F P, Nasiri M Y (2012). Prediction of the height of destressed zone above the mined panel roof in longwall coal mining. Int J Coal Geol, 98: 62–72

Mazumder S, Scott M, Jiang J (2012). Permeability increase in Bowen Basin coal as a result of matrix shrinkage during primary depletion. Int J Coal Geol, 96–97(6): 109–119

Mora C A, Wattenbarger R A (2009). Comparison of computation methods for CBM production performance. J Can Pet Technol, 48(4): 42–48

Ni X M, Jia Q F, Wang Y B (2018). Characterization of permeability changes in coal of high rank during the CH_4-CO_2 replacement process. Geofluids, 2018: 8321974

Ni X M, Jia Q F, Wang Y B (2019). The relationship between current ground stress and permeability of coal in superimposed zones of multistage tectonic movement. Geofluids, 2019: 9021586

Oskay R G, Bechtel A, Karayigit A I (2019). Mineralogy, petrography and organic geochemistry of Miocene coal seams in the Kınık

coalfield (Soma Basin-Western Turkey): insights into depositional environment and palaeovegetation. Int J Coal Geol, 210: 103205

Pillalamarry M, Harpalani S, Liu S M (2011). Gas diffusion behavior of coal and its impact on production from coalbed methane reservoirs. Int J Coal Geol, 86(4): 342–348

Prinz D, Pyckhout-Hintzen W, Littke R (2004). Development of the meso-and macroporous structure of coals with rank as analysed with small angle neutron scattering and adsorption experiments. Fuel, 83 (4–5): 547–556

Qin Y, Xu Z W, Zhang J (1995). Natural classification of the high-rank coal pore structure and its application. J China Coal Soc, 3: 266–271

Radlinski A P, Mastalerz M, Hinde A L, Hainbuchner A, Rauch H, Baron M, Lin J S, Fan L, Thiyagarajan P (2004). Application of SAXS and SANS in evaluation of porosity, pore size distribution and surface area of coal. Int J Coal Geol, 59(3–4): 245–271

Rice C A, Flores R M, Stricker G D, Ellis M S (2008). Chemical and stable isotopic evidence for water/rock interaction and biogentic origin of coalbed methane, Fort Union Formation, Powder River Basin, Wyoming and Montana USA. Int J Coal Geol, 76(1–2): 76–85

Salmachi A, Karacan C Ö (2017). Cross-formational flow of water into coalbed methane reservoirs: controls on relative permeability curve shape and production profile. Environ Earth Sci, 76(5): 200–216

Scott A R (2002). Hydrogeologic factors affecting gas content distribution in coal beds. Int J Coal Geol, 50(1–4): 363–387

Song D Y, He K K, Ji X F, Li Y B, Zhao H T (2018). Fine characterization of pores and fractures in coal based on a CT scan. Nat Gas Ind, 38(3): 41–49

Su X B, Feng Y L, Chen J F (2002). The classification of fractures in coal. Coal Geol Explor, 30(4): 21–24

Tao Y J, Zhao Y N, Xian Y S, Shi Z X, Wang Y P, Zhang W C (2020). Study of dissociation characteristics of low rank bituminous coal macerals and enhanced gravity separation. J China U Mining Technol, 49(1): 184–189

Wang G, Qin X J, Shen J N, Zhang Z Y, Han D Y, Jiang C H (2019). Quantitative analysis of microscopic structure and gas seepage characteristics of low-rank coal based on CT three-dimensional reconstruction of CT images and fractal theory. Fuel, 256: 115900

Yang Y H, Meng Z P, Chen Y J, Yang Y L, Gan D Y (2015). Geo-stress condition of coal reservoirs in Qinnan-Xiadian block and its influences on permeability. Acta Petrol Sin, 36(S1): 91–96

Yang Z B, Zhang Z G, Qin Y, Wu C C, Yi T S, Li Y Y, Tang J, Chen J (2018). Optimization methods of production layer combination for coalbed methane development in multi-coal seams. Pet Explor Dev, 45(2): 312–320

Yang Z B, Li Y Y, Qin Y, Sun H S, Zhang P, Zhang Z G, Wu C C, Li C L, Chen C X (2019a). Development unit division and favorable area evaluation for joint mining coalbed methane. Pet Explor Dev, 46(3): 583–593

Yang Z B, Peng H, Zhang Z G, Ju W, Li G, Li C L (2019b). Atmospheric-variational pressure-saturated water characteristics of medium-high rank coal reservoir based on NMR technology. Fuel, 256: 115976

Yang Z B, Qin Y, Wu C C, Qin Z H, Li G, Li C L (2019c). Geochemical response of produced water in the CBM well group with multiple coal seams and its geological significance—a case study of Songhe well group in western Guizhou. Int J Coal Geol, 207: 39–51

Yao Y B, Liu D M (2012). Comparison of low-field NMR and mercury intrusion porosimetry in characterizing pore size distributions of coals. Fuel, 95: 152–158

Yao Y B, Liu D M, Che Y, Tang D Z, Tang S H, Huang W H (2009). Non-destructive characterization of coal samples from China using microfocus X-ray computed tomography. Int J Coal Geol, 80(2): 113–123

Yao Y B, Liu D M, Tang D Z, Tang S H, Huang W H (2010 a). Influence and control of coal petrological composition on the development of microfracture of coal reservoir in the Qinshui Basin. J China U Min Technol, 39(1): 6–13

Yao Y B, Liu D M, Che Y, Tang D Z, Tang S H, Huang W H (2010b). Petrophysical characterization of coals by low-field nuclear magnetic resonance (NMR). Fuel, 89(7): 1371–1380

Yu S, Jiang B, Li M, Hou C L, Xu S C (2020). A review on pore-fractures in tectonically deformed coals. Fuel, 278: 118248

Zhang S H, Tang S H, Tang D Z, Pan Z J, Yang F (2009). The characteristics of coal reservoir pores and coal facies in Liulin district, Hedong coal field of China. Int J Coal Geol, 80(2): 113–123

Zhang Y, Lebedev M, Al-Yaseri A, Yu H, Xu X, Sarmadivaleh M, Barifcani A, Iglauer S (2018). Nanoscale rock mechanical property changes in heterogeneous coal after water adsorption. Fuel, 218: 23–32

Zhao J, Tang D, Qin Y, Xu H, Liu Y, Wu H (2018). Characteristics of methane (CH_4) diffusion in coal and its influencing factors in the Qinshui and Ordos basins. Energy Fuels, 32(2): 1196–1205

Zhao S H, Li Y, Wang Y B, Ma Z T, Huang X Q (2019). Quantitative study on coal and shale pore structure and surface roughness based on atomic force microscopy and image processing. Fuel, 244: 78–90

Zhao Y X, Liu S M, Elsworth D, Jiang Y D, Zhu J (2014). Pore structure characterization of coal by synchrotron small-angle X-ray scattering and transmission electron microscopy. Energy Fuels, 28(6): 3704–3711